Deep-Sea Research II 57 (2010) 5–26

Contents lists available at ScienceDirect

Deep-Sea Research II

journal homepage: www.elsevier.com/locate/dsr2

Evolution and dynamics of the flow through Herald Canyon in the western Chukchi Sea

Robert S. Pickart [a,*], Lawrence J. Pratt [a], Daniel J. Torres [a], Terry E. Whitledge [c], Andrey Y. Proshutinsky [a], Knut Aagaard [b], Thomas A. Agnew [d], G.W.K. Moore [e], Holly J. Dail [a]

[a] Woods Hole Oceanographic Institution, Woods Hole, MA 02540, USA
[b] Applied Physics Laboratory, University of Washington, Seattle, WA 98105, USA
[c] School of Fisheries and Oceans, University of Alaska, Fairbanks, AK 99775, USA
[d] Meteorological Service of Canada, Downsview, OT, Canada M3H 5T4
[e] University of Toronto, Toronto, OT, Canada M5S 1A1

ARTICLE INFO

Available online 11 August 2009

Keywords:
Arctic canyons
Canyon dynamics
Pacific winter water
Hydraulics
Polynyas

ABSTRACT

The flow of summer and winter Pacific water masses through Herald Canyon is investigated using data from a high-resolution hydrographic/velocity survey conducted in summer 2004. The survey was part of the Russian-American Long Term Census of the Arctic (RUSALCA) program, and consisted of four cross-canyon transects occupied over a 2-day period. At the time of the survey dense winter water was entering the western side of the canyon from the Chukchi Sea, flowing alongside a poleward jet of summer water on the canyon's eastern flank. As the dense water progressed northward it switched sides of the canyon and underwent a sudden increase in layer thickness. This coincided with vertical mixing near the interface of the winter and summer water, producing a new water mass mode exiting the canyon. All of these features are consistent with the notion of hydraulic activity occurring in the canyon. A three-layer hydraulic theory is applied to the flow, which suggests that it is supercritical and that hydraulic control is likely. A lock-exchange formulation accurately predicts the northward transport of the winter water. The origin of the winter water and the manner in which it drains into the canyon is investigated using satellite ice-concentration data, atmospheric re-analysis fields, historical in-situ data, and a simple circulation model. Finally, the fate of the Pacific water exiting the canyon, and its connection to the Chukchi shelfbreak current, is discussed.

1. Introduction

In order for Pacific water to reach the interior basin of the Arctic Ocean it must first cross the wide and shallow Chukchi Sea north of Bering Strait. Numerical models suggest differing degrees of topographic steering of the flow as it progresses northward on the shelf. In the barotropic model of Winsor and Chapman (2004) the inflow from Bering Strait spreads out across the Chukchi Sea, with some areas of intensification due to specific bathymetric features. By contrast, the depth-averaged streamlines in Spall's (2007) model show three distinct branches of Pacific water north of the strait (shown schematically in Fig. 1): in the western Chukchi Sea through Herald Canyon, in the eastern Chukchi Sea through Barrow Canyon, and on the central shelf through the channel between Hanna and Herald shoals (known as the Central Channel, Weingartner et al., 2005). Presently there are not enough observations to pin down the precise mean circulation of the Chukchi Sea, but the evidence to date suggests that the bulk of the 0.8 Sv ($1\,\mathrm{Sv} = 10^6\,\mathrm{m^3\,s^{-1}}$) of Pacific water flowing northward through Bering Strait is carried toward the shelf-edge in distinct branches. This includes the three branches noted above, plus a fourth branch through Long Strait (Woodgate et al., 2005). This latter pathway does not appear in the above models, possibly because of the closed western boundary in each of the simulations. On the other hand, Woodgate et al. (2005) had only a single mooring with which to estimate the net transport through Long Strait, so the volume transport of this branch is uncertain. However, the Long Strait branch is a known pathway for nutrients into the East Siberian Sea (Codispoti and Richards, 1968), and synoptic velocity measurements in summer have revealed northwestward flow of Pacific water through the strait (Weingartner et al., 1999).

One well-known aspect regarding the circulation of the Chukchi Sea is that the two canyons at the shelf-edge significantly influence the northward flow of Pacific water, resulting in two areas of enhanced outflow (Coachman et al., 1975). Consequently,

* Corresponding author.
E-mail address: rpickart@whoi.edu (R.S. Pickart).

0967-0645/$ - see front matter © 2009 Elsevier Ltd. All rights reserved.
doi:10.1016/j.dsr2.2009.08.002

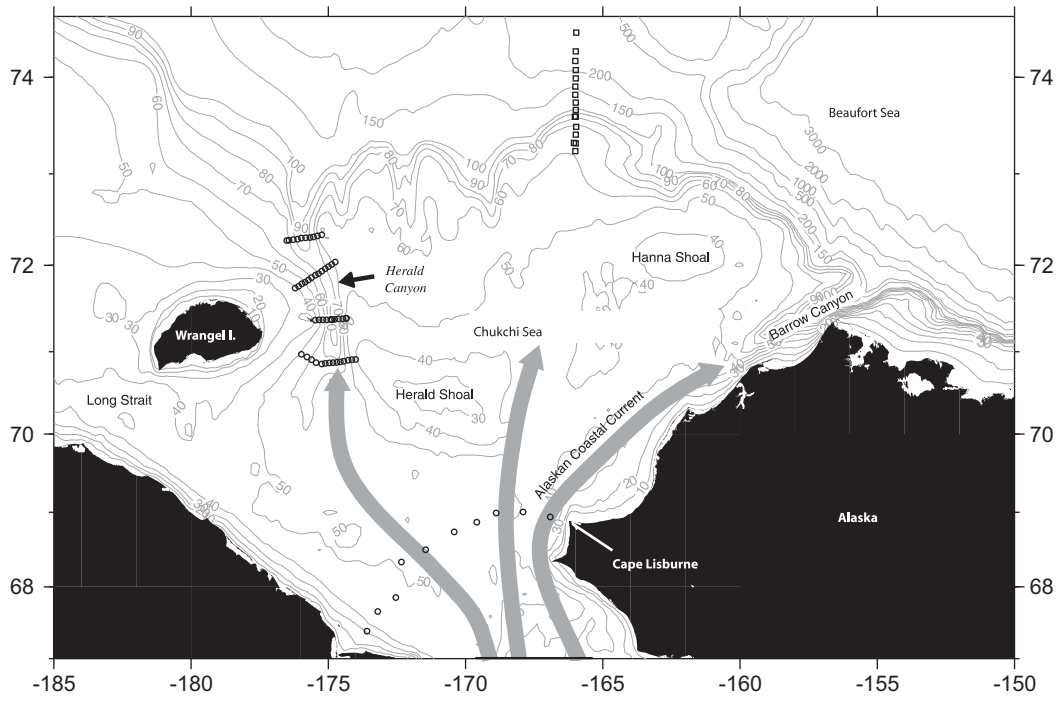

Fig. 1. Study area of the Chukchi Sea, including names of geographical features. Three branches of the Bering Strait inflow are represented schematically, the western-most of which feeds Herald Canyon. Circles denote stations occupied as part of the RUSALCA program in August 2004. The four transects in Herald Canyon are the focus of the paper. Also shown is the section across the Chukchi slope at 166°W (squares), occupied in September 2004 as part of the Western Arctic Shelf-Basin Interactions (SBI) program.

these regions are of particular importance for understanding the impacts that the shelf-derived waters have on the interior Arctic basin, including the ventilation of the cold halocline and the offshore flux of nutrients, carbon, and zooplankton. As summarized in Pickart et al. (2005), Barrow Canyon, on the northeast Chukchi shelf, has been studied extensively, and there is a significant body of literature describing various aspects of the canyon flow and the water masses within it. This includes the role of winds and upwelling (e.g. Aagaard and Roach, 1990), the impact of polynyas (e.g. Weingartner et al., 1998), and the vorticity dynamics as they relate to eddy formation (D'Asaro, 1988; Munchow and Carmack, 1997; Pickart et al., 2005). By contrast, comparatively little is known about Herald Canyon, on the northwest Chukchi shelf. For example, while numerous mooring records have been obtained in Barrow Canyon over the years (e.g. Garrison and Becker, 1976; Aagaard and Roach, 1990; Weingartner et al, 1998, 2005), only a single long-term mooring record exists for Herald Canyon (Woodgate et al., 2005).

Nonetheless, previous shipboard programs and historical data analyses have shed light on some aspects of the flow through Herald Canyon. Significant differences seem to exist between the two sides of the canyon, both in terms of the water masses and the currents. As mentioned above, this canyon is one of the main conduits for the flow emanating from Bering Strait (Coachman et al., 1975). For the most part, the Bering Sea-origin water in this branch is believed to flow along the eastern flank of the canyon. In winter this consists of cold, salty winter-transformed Pacific water originating from the Bering Sea (Muench et al., 1988), modified further by cooling and brine-rejection within the Chukchi Sea (Weingartner et al., 1998; Woodgate et al., 2005). In summer, the flow in this branch is mainly summertime Bering Sea Water (Coachman et al., 1975),[1] which is separated by a frontal boundary from the water masses in the western portion of Herald Canyon (Coachman et al., 1975; Kirillova et al., 2001; Weingartner et al., 2005).

What is the source of water on the western side of Herald Canyon? In the near-surface layer Weingartner et al. (2005) observed a cold and fresh water mass during summer, believed to result from ice-melt, on three different cruises from 1993 to 1995. The deep layer seems to consist of winter-transformed water throughout much of the year (Kirillova et al., 2001; Weingartner et al., 2005; Woodgate et al., 2005). Weingartner et al. (2005) state that this deep water mass is simply the resident Chukchi Sea winter water (which in summer is a remnant from the previous winter), while Kirillova et al. (2001) refer to it as a "Wrangel type" of water mass. This terminology implies that the formation region is near Wrangel Island, where in wintertime it is well known that persistent polynyas form in the lee of the island (Cavalieri and Martin, 1994; Winsor and Björk, 2000), producing brine-enriched bottom water (e.g. Weingartner et al., 1998). There is evidence of such polynya-driven water formation in the Long Strait mooring record of Woodgate et al. (2005).

As is the case with the water masses, there also seem to be distinct flow regimes on either side of Herald Canyon. A year-long current meter record from 1990 to 1991 obtained from the canyon's eastern flank showed predominantly northward flow (with reduced amplitude in winter), consistent with the idea of a direct route from Bering Strait to this side of the canyon (Woodgate et al., 2005). By contrast, the corresponding current meter record from the western flank showed weaker and more variable flow (although this record ended after only 3.5 months). These differences are mirrored in the summertime shipboard velocity data presented by Weingartner et al. (1999), which showed persistent strong northward flow on the eastern flank, and sluggish, variable flow on the western flank. If the flow on the western flank is not part of the Bering Strait branch that passes through the canyon, then what forces it? Kirillova et al. (2001) postulate a scenario in which the Wrangel-origin dense water flows northward into the Arctic basin during winter on the

[1] Also referred to as western Chukchi Summer Water (Shimada et al., 2001).

western side of the canyon, while in summer the same water mass flows southward back into the canyon. Coachman et al. (1975) note the possibility of dense water flowing northward on the east side of Wrangel Island, having originated from Long Strait. Finally, local or remote winds may impact the currents. Wind-forced upwelling of deep Atlantic water into Barrow Canyon is common (e.g. Mountain, 1974), and Coachman et al. (1975) speculate that this happens as well in Herald Canyon. Interestingly, the currents measured in 1990–1991 on the eastern flank were not significantly correlated with the local winds (Woodgate et al., 2005), although there were numerous episodes of up-canyon flow during the fall and winter months.

This paper presents results from a hydrographic/velocity survey conducted in Herald Canyon in summer 2004. The goal of the experiment was to quantify the evolution of the flow through the canyon, in order to help shed light on how the canyon geometry and dynamics might influence the properties and transport of the Pacific water as it enters the deep Arctic basin. To meet this goal, a set of four high-resolution transects were occupied across the canyon (Fig. 1), which to our knowledge is the first such survey in Herald Canyon to sample at the scale of the Rossby radius of deformation (order 5 km at this latitude). These measurements revealed a heretofore unknown flow regime involving the interaction of northward-flowing summer and winter water masses, characterized by the transposition of the dense water from the western side of the canyon to the eastern side. The paper is organized as follows. After presenting the data set, the evolution of the water masses and currents through the canyon is described. This is followed by a discussion of the possible dynamical causes of the observed changes from the head of the canyon to its mouth. Finally, the source of the dense water feeding the western side of the canyon is investigated, and the far-field signature of the canyon outflow on the shelf-edge boundary current of the Chukchi Sea is considered.

2. Data and methods

From 9 to 24 August, 2004 the research vessel *Professor Khromov* carried out a multidisciplinary survey of the Chukchi Sea, including biological, chemical, and physical sampling of the water column and benthos. This was the second leg of the inaugural cruise of the Russian-American Long-Term Census of the Arctic (RUSALCA) program. After completing measurements in the southern Chukchi Sea, the *Khromov* occupied a set of four transects in Herald Canyon (Fig. 1). The canyon survey took just under 2 days to complete, and the cross-stream station spacing was approximately 5 km, which was necessary to resolve the complex cross-canyon water mass and velocity structure. The survey represented a quasi-synoptic snapshot in that, based on the velocity measurements, a water parcel traveling with the swiftest part of the flow took more than 5 days to travel from the canyon's head to its mouth at the time of the survey. The winds before and during the survey were weak (less than 4 m s^{-1} from the south, based on the National Centers for Environmental Prediction (NCEP) re-analysis fields), and the pack-ice concentration in the canyon was generally 10%, with a few isolated areas of approximately 50% concentration (based on visual observations during the cruise).

2.1. Instrumentation

The conductivity/temperature/depth (CTD) package consisted of a SeaBird SBE911+, with a dissolved oxygen sensor, transmissometer, fluorometer, and altimeter. These were mounted on a 21-position rosette with 10 l bottles; along with a dual 300 kHz RDI Workhorse lowered acoustic Doppler current profiler (ADCP) system. Water samples were collected for measurements of salinity and nutrients. To determine the latitude and longitude of the CTD stations, and to calculate the barotropic component of the lowered ADCP velocity profiles, a GPS instrument was mounted on the 02 deck of the *Khromov*. The instrument was a Garmin model GPSMAP 182/232 12-channel parallel receiver, with an accuracy of approximately 4 m. Station bottom depths were computed using the altimeter on the CTD package.

The CTD downcast data were run through standard post-acquisition processing routines to produce 1-db averaged files. The accuracy of the temperature measurements, based on pre- and post-cruise laboratory calibrations, is 0.002 °C. Because all of the stations were occupied in relatively shallow water (where vertical property gradients are generally large) the bottle data could not be used to perform a reliable in-situ salinity calibration. To assess the accuracy of the CTD salinity measurements, we regressed the values obtained by the dual sensors against each other (excluding depths shallower than 10 m). After an initial regression line was determined, all values outside the three standard deviation envelope were discarded (which removed 4% of the points), and the regression was calculated again. The standard deviation of the resulting scatter, which is taken as a rough measure of the salinity accuracy, was 0.008. Derived variables were computed from the CTD profiles, including potential temperature (θ), potential density (σ_θ), buoyancy frequency (N), and Richardson Number (Ri). For the nutrient analysis, the samples were collected in polyethylene scintillation vials and immediately capped and stored in a dark refrigerator. Within 2 h after collection, inorganic nitrate, ammonium, silicate, and phosphate concentrations were analyzed using an automated nutrient analyzer (Alpkem RFA model 300) following the methods of Whitledge et al. (1981). The accuracy of the nutrient measurements is $\pm$0.2%, with a full-scale range of 5 V.

The lowered ADCP data were processed using the Lamont-Doherty Earth Observing System software, using 5-m bins. Based on the accuracy of the GPS unit, the barotropic velocity error is approximately 1 cm s^{-1}. The calculated uncertainty in the velocity shear increases the overall velocity error to approximately 4 cm s^{-1}. However, based on previous cruises when vessel-mounted ADCP data were available for comparison, we believe that the lowered ADCP velocity profiles have a higher degree of accuracy than this (there was no vessel-mounted ADCP on the *Khromov*). The velocity data were subsequently de-tided using the Oregon State University 1/12° Arctic model (Padman and Erofeeva, 2004). These results were compared with the output from the Kowalik and Proshutinsky (1993) tidal model, and the differences were found to be small.

Vertical sections of the CTD variables were constructed using Laplacian-Spline interpolation with a grid spacing of 2.5 km in the horizontal and 2 m in the vertical. Sections of absolute geostrophic velocity were also constructed for each of the canyon transects. This was done by using the gridded fields of temperature and salinity to compute thermal wind velocities, and referencing these to the gridded lowered ADCP along-canyon velocity sections. The matching was done at each horizontal grid point using the water column-averaged flow. We note that the along-canyon velocity sections computed using only the lowered ADCP data are qualitatively similar to the absolute geostrophic velocity sections, indicating that the final processed lowered ADCP measurements were not significantly contaminated by tides or other ageostrophic motions.

2.2. Ancillary data

Additional data were used in various parts of the study. This included a hydrographic section from the Western Arctic Shelf-Basin

Interactions (SBI) program occupied across the Chukchi shelfbreak and slope about one month after the Herald Canyon survey (Fig. 1). We also used historical hydrographic and current meter data from the vicinity of the canyon collected in 1990–1991. NCEP 6-hourly reanalysis fields, run through the heat flux correction scheme of Moore and Renfrew (2002), were used to address the atmospheric forcing. Sea-ice concentration fields, constructed using output from the Advanced Microwave Scanning Radiometer-Earth Observing System (AMSR-E), were analyzed to investigate polynya activity near Wrangel Island. The NASAteam algorithm was used on the 19 and 37 GHz vertical and horizontal polarization channels of the passive microwave data in order to make the ice-concentration images. This algorithm is deemed accurate to $\pm 10\%$ of the actual sea-ice concentration (e.g. Cavalieri et al., 1991). The native resolution of the AMSR-E sensor is 12.5 km, and we interpolated these data to 6.25 km.

3. Evolution of flow through the canyon

3.1. Water masses and velocity

At the time of the survey, both winter water (defined here as $-1.85\,^{\circ}\mathrm{C} \le \theta \le -1.65\,^{\circ}\mathrm{C}$) and summer water ($-1.0\,^{\circ}\mathrm{C} \le \theta \le 4.0\,^{\circ}\mathrm{C}$) were present in the canyon. The predominant flow of both water masses was northward, and there was significant evolution of the water properties and currents from the head of the canyon to its mouth (Figs. 2–4). At the head of the canyon (Figs. 2B and 3B) one sees a strong jet of summer water ($>50\,\mathrm{cm\,s^{-1}}$) in the eastern/central parts of the canyon, presumably advecting water from Bering Strait along the Herald Canyon flow branch discussed in the introduction and shown schematically in Fig. 1. This warm water is separated by a sharp temperature front from cold, dense winter water on the western side of the canyon that flows northward more slowly ($5–10\,\mathrm{cm\,s^{-1}}$). Away from the front the stratification in the deep water is weak (both in the warm and cold water), capped by a seasonal pycnocline at 10–20 m. The velocity field on both sides of the canyon is generally barotropic, and the lateral shear between the fast-moving summer water and slower-moving winter water results in a fairly large value of relative vorticity, $\zeta/f \sim 0.25$ (where ζ is dominated by the cross-stream gradient of the along-canyon velocity, and f is the Coriolis parameter). This suggests that non-linear effects could be important in the evolution of the poleward flow.

Progressing northward (Figs. 2C and 3C), the sides of the canyon become steeper and the poleward flow responds accordingly. At this location the winter water is an isolated lens along the western flank, much like what is observed in Denmark Strait as the dense Norwegian-Greenland overflow water descends into the Irminger Sea (Smith, 1975). The jet of summer water has slowed somewhat (although it is likely that the eastward-most portion of the jet was not sampled by the section, see below), and there is now a weak up-canyon flow on the western edge of the canyon. The remaining transects (Figs. 2D, E and 3D, E) reveal that the northward-flowing winter water switches sides of the canyon from the western flank to the eastern flank by the time it reaches the canyon mouth (the axis of the canyon is marked by the arrow in each panel). The ramifications of this are significant: if the dense outflow that ultimately emerges from the canyon follows topographic contours, it will turn to the right along the continental slope and flow eastward toward the Beaufort Sea, instead of heading to the west towards the East Siberian Sea. The reasons for the observed transposition of the dense water in the canyon are explored below. Note also that the swift jet on the eastern side of the canyon, advecting summer water in the southern three transects, has cooled considerably by Section 4 (again not all of the jet has been sampled). In particular, the core of the jet (near station 81) is colder than $-1\,^{\circ}\mathrm{C}$. This temperature change is considered in more detail as well below. As with Section 2, the northern two transects have up-canyon flow on the western flank of the canyon. Finally, the evolution of salinity is shown in Fig. 4. This indicates that the winter water being advected through the canyon corresponds to that found in the upper halocline of the interior Arctic basin. This is elaborated on in the discussion section.

3.2. Nutrients

Although the nutrient data are more sparse, they shed light on the origins of the water masses in the canyon and the biological processes at work. Fig. 5 shows the distribution of silicate through the canyon (colored symbols). One sees that the winter water (shaded gray) is characterized by high concentrations of silicate (true for phosphate and nitrate as well, not shown). This nutrient signature was likely acquired during the dense water formation process. When ice is formed, the rejection of brine into the surface water column leads to convection which, on the shallow shelf, is known to reach the bottom. This can re-suspend the nutrients that are present in the sediment pore water. A more minor effect may be due to the rejection of nutrients directly from the ice along with the brine. Silicate is the best tracer of the winter Pacific water in the Arctic because of its high signal to noise ratio compared to the surrounding water, and due to the fact that it is more conservative than other nutrients such as nitrate (which is transformed more readily by bacteria).

As expected, the nutrient levels in the surface layer are nearly depleted due to the spring and summer phytoplankton blooms. The particularly low levels of nitrate, in conjunction with low ammonium in the surface layer (not shown), imply that, overall, the bloom was nitrate limited. As seen in Fig. 5, the silicate concentrations are also low in the summer water at depth. This is likely because primary productivity had been occurring on the Chukchi shelf for a long enough time before the August survey (3 months or so) for nutrient draw-down to take place as deep as 50 m or so. This is consistent with the primary production data obtained during RUSALCA, reflecting in part the very clear water in the upper part of the water column. According to the model results of Winsor and Chapman (2004), three months is roughly the time it takes for a water parcel to travel from Bering Strait to the eastern side of Herald Canyon (keeping in mind that the winds in summer tend to be weak and westerly, Weingartner et al., 1998). This in turn should provide time for a portion of the phytoplankton mass to sink to the benthos, consistent with the discussion of the bottom boundary layer presented below.

3.3. Layer averages

To shed more light on the evolution of the winter water through Herald Canyon, we made lateral maps of different properties within the dense layer. To do this, a Cartesian coordinate system was constructed surrounding the canyon (Fig. 6A). To get the bottom topography, the International Bathymetric Chart of the Arctic Ocean (IBCAO version 1.0) data were transformed to this grid. The resolution of IBCAO is 2.5 km, but we found significant differences between the interpolated IBCAO bottom depths at the station sites and the values calculated using the CTD pressure and altimeter data. For this reason, the CTD-derived bottom depths were used to construct the topographic contours of Fig. 6. We defined the winter water layer to be that part of the water column denser than $26.2\,\mathrm{kg\,m^{-3}}$ and colder than -1.65 °C (cf. Fig. 2B).

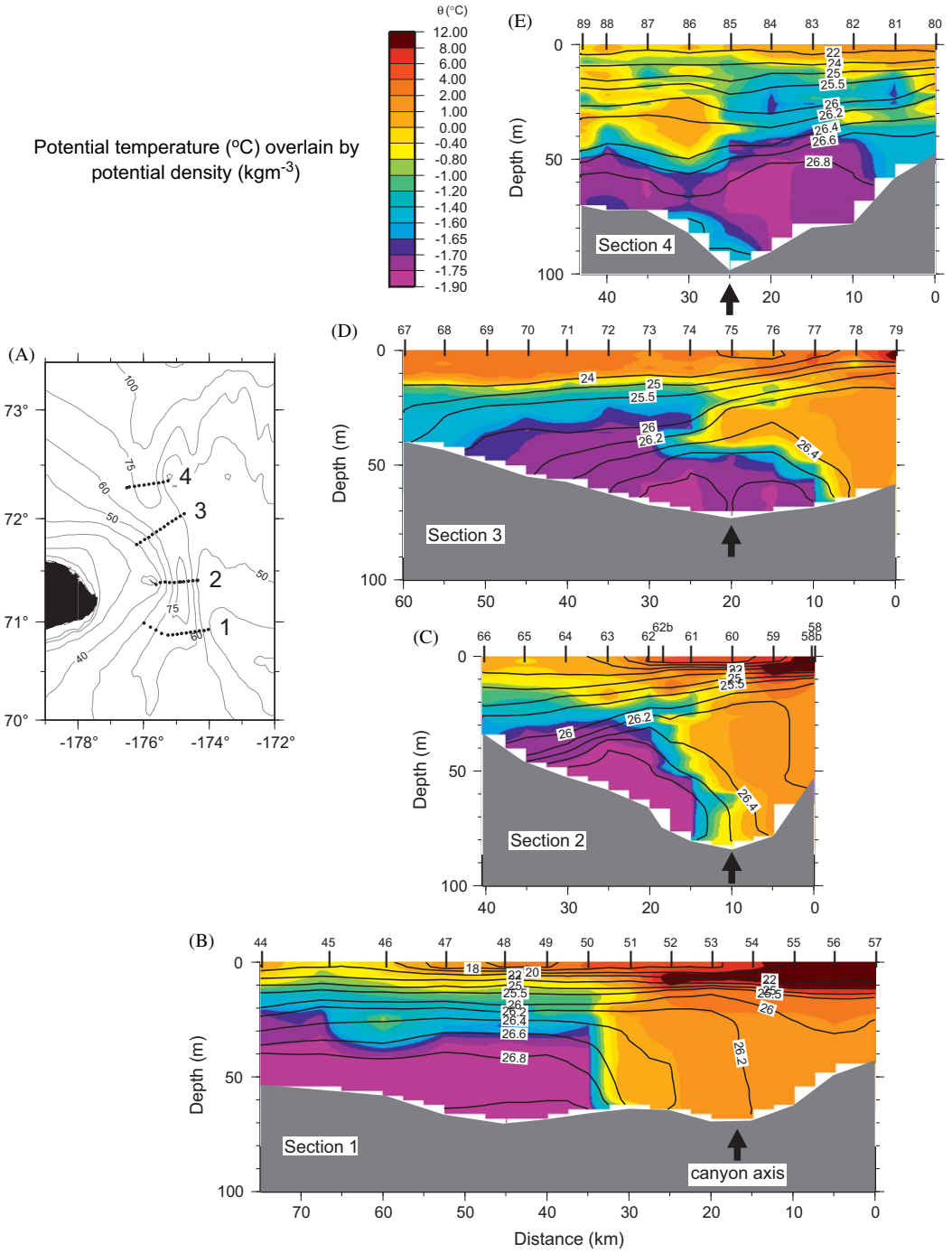

Fig. 2. Evolution of the water masses from south to north in Herald Canyon. The vertical sections are oriented such that the viewer is looking north, and the sections are positioned so that the center of the canyon is aligned (as indicated by the arrows). (A) Locations of the four transects. (B)–(E) Potential temperature (color) overlain by potential density (contours). Station numbers are indicated along the top. (For interpretation of the references to color in this figure legend, the reader is referred to the web version of this article.)

The distributions of potential temperature, turbidity, and layer thickness for the winter water layer defined above are shown in Fig. 6. This demonstrates clearly that the coldest water draining into Herald Canyon from the Chukchi Sea switches sides of the canyon (and warms slightly, Fig. 6A). It also shows that the winter water, although high in nutrients, is relatively low in turbidity as it enters the canyon. However, as the water crosses to the eastern flank, the turbidity increases significantly (Fig. 6B). This may be due to a difference in the bottom sediments on this side of the canyon, but, as discussed below, the dynamics of the bottom boundary layer may be partly responsible for the increase in suspended particles. The thickness of the winter water layer (Fig. 6C) displays an interesting distribution, with larger values at the two ends of the canyon. An increased layer thickness upstream is consistent with the notion of a reservoir of dense water draining into the canyon, which would presumably thin out as the water accelerates downstream. However, the reason for the increase in layer thickness near the mouth of the canyon is not obvious; it may also be the result of the dynamics of the flow, as addressed below in the discussion on hydraulics.

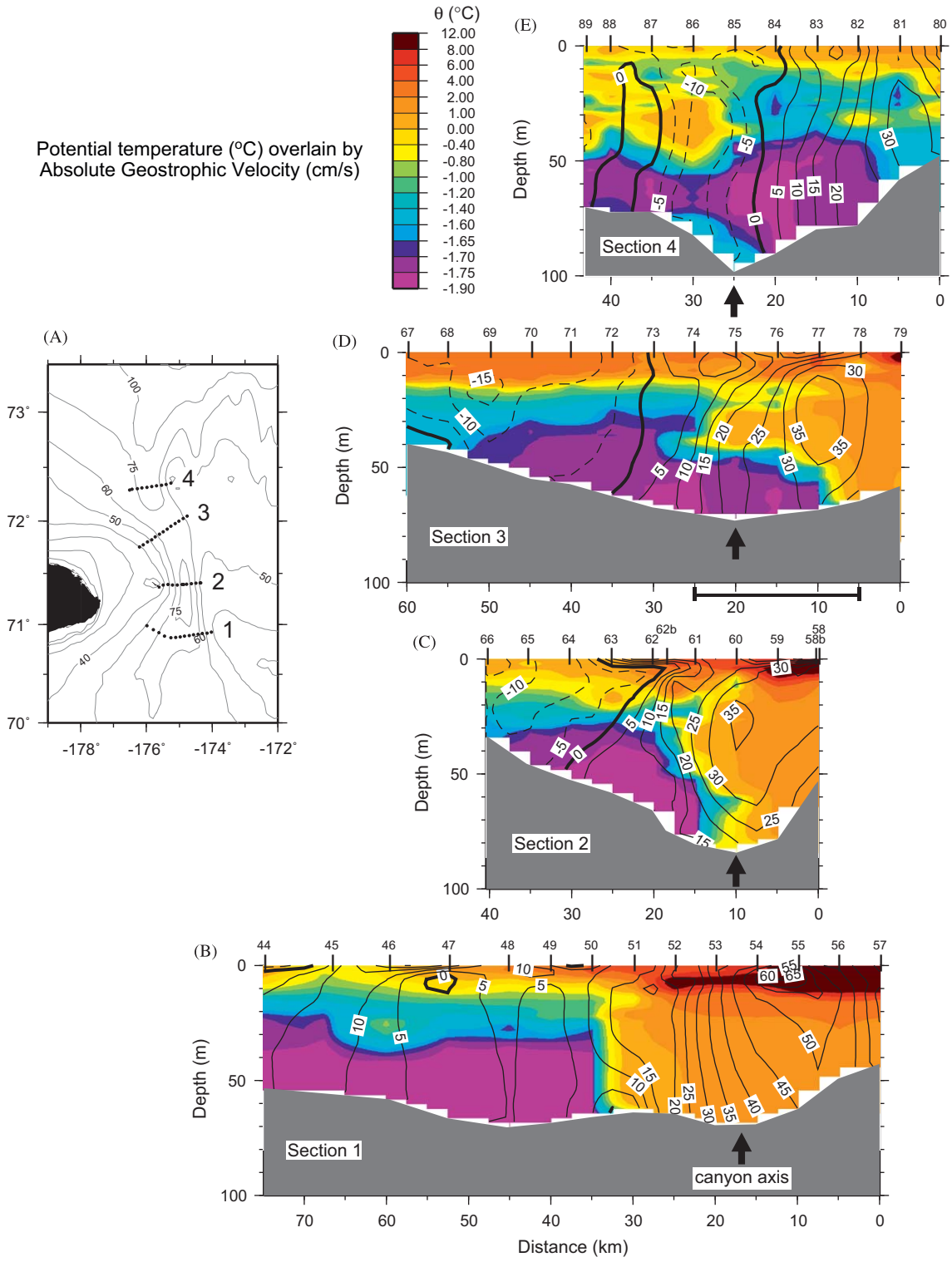

Fig. 3. Evolution of the water masses and flow field from south to north in Herald Canyon. The presentation is the same as in Fig. 2. The contours in (B)–(E) are absolute geostrophic velocity (positive denotes northward flow). The core of the poleward flow at Section 3, considered in the hydraulic analysis, is marked by the bar along the horizontal axis in (D).

3.4. Volume transport

The volume transports across each of the transects, subdivided by water class, are presented in Table 1. Included are the total transport, as well as the transport of the summer water, winter water, and an intermediate water class (described shortly). One immediately sees that mass is not conserved, with a considerable reduction (approximately 0.6 Sv) in the northward volume flux from the head of the canyon to the mouth. This is possibly because the sections did not extend far enough to the east to capture all of the poleward-flowing summer water (Fig. 3). Another possibility is that the flow on the eastern side of the

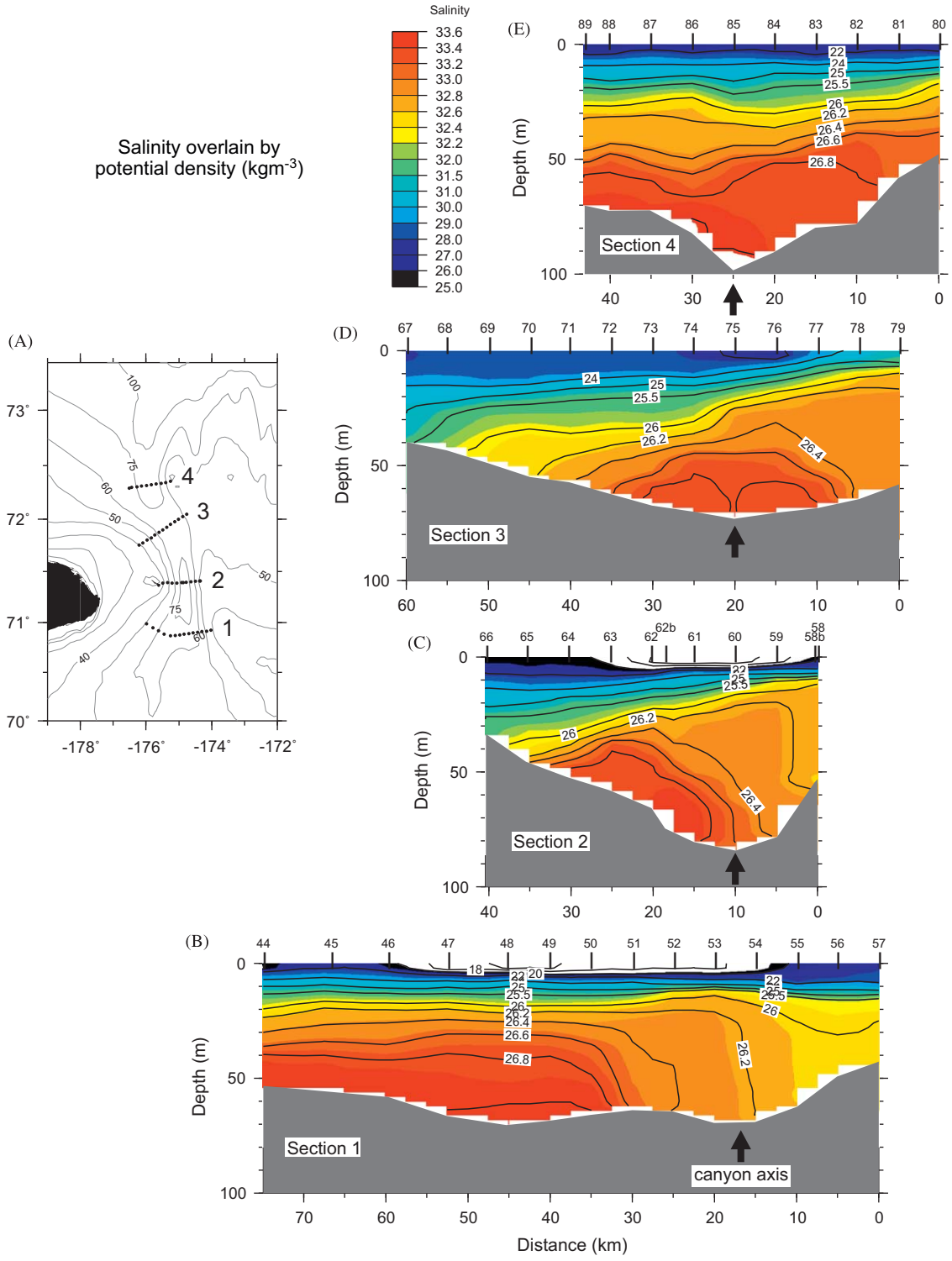

Fig. 4. Evolution of the water masses from south to north in Herald Canyon. The presentation is the same as in Fig. 2, except for salinity (color). (For interpretation of the references to color in this figure legend, the reader is referred to the web version of this article.)

canyon is diverted into the central Chukchi Sea as one progresses northward through the canyon. This might be expected based on the topography of Herald Shoal (Fig. 1). In particular, note how the 40 and 50 m isobaths curve to the east away from Herald Canyon, so that any geostrophic flow in contact with the bottom should do the same. This is the case in the numerical models of Winsor and Chapman (2004) and Spall (2007) (see also Fig. 15). In any event, the measured drop in transport of the summer water (approximately 0.5 Sv) accounts for most of the overall reduction in northward transport. By contrast, the flux of winter water remained relatively constant through the canyon (0.08 ± 0.026 Sv). Note that the up-canyon (southward) transport is generally small (and zero at the head of the canyon).

From inspection of Table 1 it is tempting to conclude that the northward jet of summer water was completely missed at the northern-most section. However, Fig. 3E reveals that, in fact, the

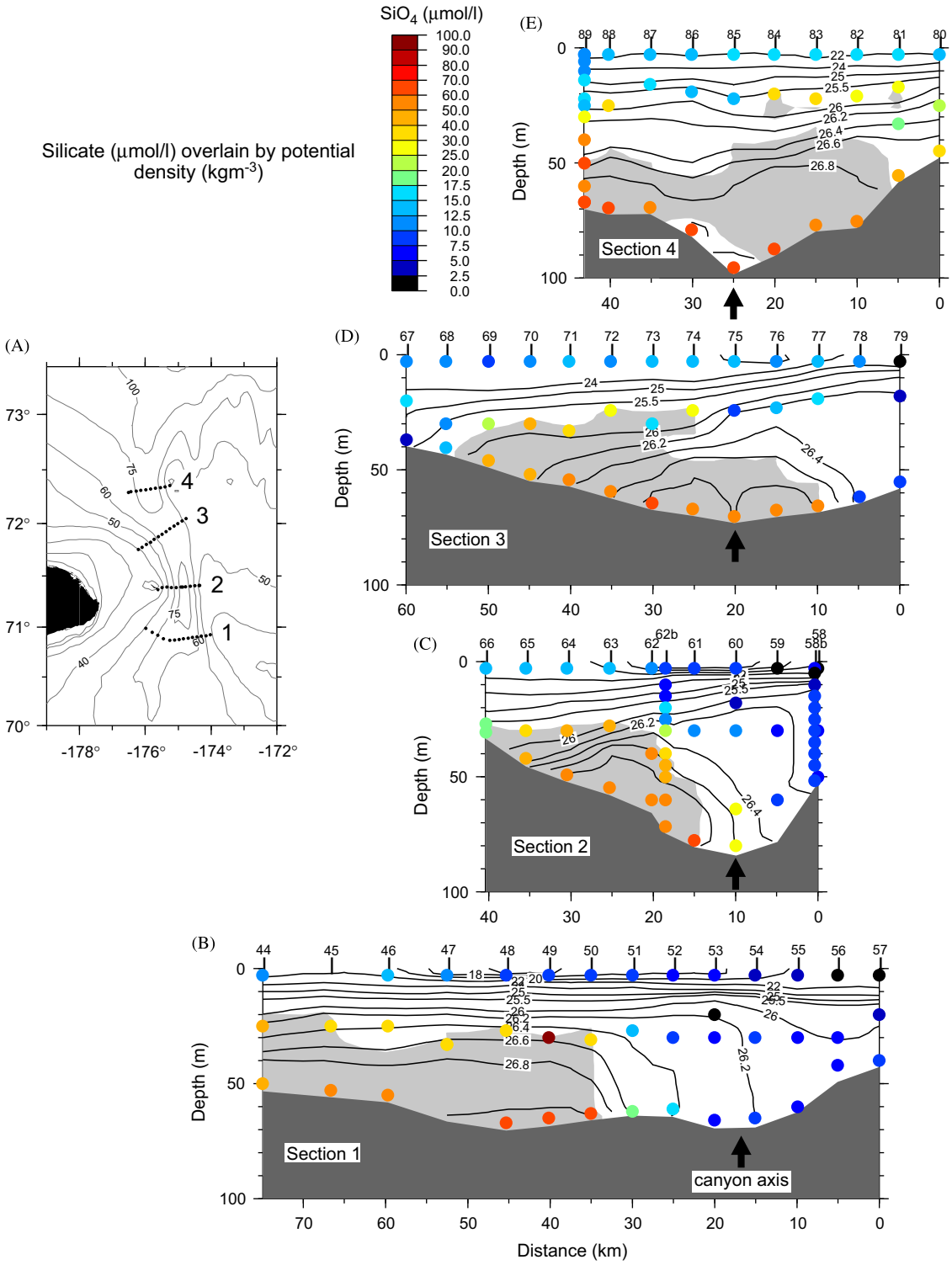

Fig. 5. Evolution of the silicate distribution from south to north in Herald Canyon. The presentation is the same as in Fig. 2. The colored circles in (B)–(E) denote SiO_4 concentration, overlain by potential density (contours). The gray shading denotes the winter water (potential temperature $\leq -1.6\,^{\circ}C$). (For interpretation of the references to color in this figure legend, the reader is referred to the web version of this article.)

section extended far enough to the east to capture the core of the jet. However, the temperature of the water comprising the jet has cooled considerably. To shed light on this it is useful to display the volume transport in T/S space (Fig. 7). This reveals clearly that the two dominant transport modes are the summer water and winter water. These modes are present at Sections 1–3, but by section 4 the summer mode is absent. However, a separate, intermediate mode (somewhat warmer and fresher than the winter mode) appears at section 4, which geographically is associated with the core of the jet on the eastern side of the canyon. Table 1 shows this enhancement of intermediate water transport, which, at the exit of the canyon, is comparable to the flux of winter water. Hence, while the hydrographic survey may have missed a significant portion of the northward-flowing summer water (or some of the

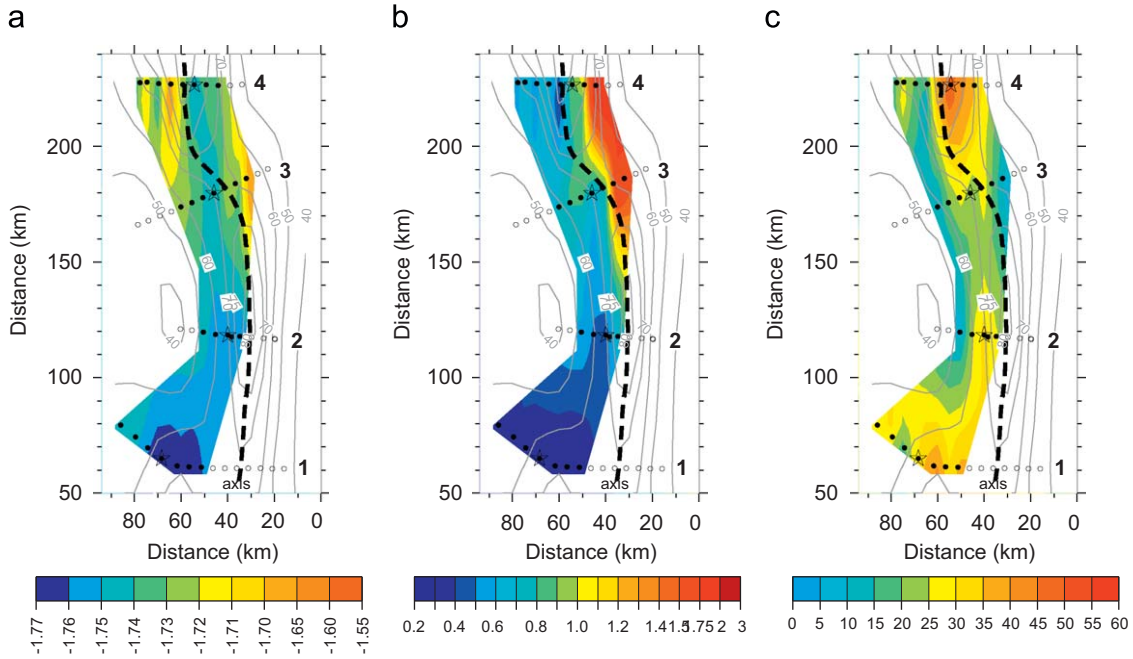

Fig. 6. Plan view of average properties in the winter water layer (color). (A) Potential temperature; (B) turbidity; (C) layer thickness. Bottom depths (contours) were obtained using the altimeter on the CTD package. The sites where the layer was present are indicated by the closed circles, and the remaining sites are denoted by open circles. The canyon axis is marked by the thick dashed line. The stations in the core of the dense outflow that were used for Fig. 9 are indicated by the stars. (For interpretation of the references to color in this figure legend, the reader is referred to the web version of this article.)

Table 1
Volume transport (in Sv) across the four sections, including the full water column and individual water masses (see text).

	Full water column (Sv)		Summer water (Sv)		Winter water (Sv)		Intermediate water (Sv)		Residual (Sv)	
	N	S	N	S	N	S	N	S	N	S
Section 1	+0.89	0	+0.56	0	+0.09	0	+0.03	0	+0.21	0
Section 2	+0.42	−0.06	+0.28	0	+0.04	0	+0.04	0	+0.06	−0.06
Section 3	+0.47	−0.11	+0.28	0	+0.10	−0.01	+0.03	−0.01	+0.06	−0.09
Section 4	+0.28	−0.09	+0.03	−0.03	+0.08	−0.02	+0.10	−0.02	+0.07	−0.02

Northward transport (N) is positive, and southward transport (S) is negative.

water was diverted eastward onto the Chukchi shelf), a new transport mode was established in the canyon.

We argue below that the transposition of the winter water from the western flank of the canyon to the eastern flank, the evolution of layer thickness of the winter water, its volume flux, as well as the establishment of the new transport mode, are consistent with hydraulic behavior in Herald Canyon.

4. Hydraulics, mixing, and frictional effects

The descending flow of winter water observed between Sections 1 and 4 shares at least two features with the overflows of the Denmark Strait, Faroe-Bank Channel, and other hydraulically driven sill flows in the ocean. One is the shift in the position of the dense water from the left wall to the right wall (facing downstream) as it descends the Canyon (Fig. 3). This behavior is seen in rotating hydraulic models (e.g. Whitehead et al., 1974 and Gill, 1977) that treat the overflow as a single-layer, and has been observed in the Denmark Strait overflow (e.g. Nikolopoulos et al., 2003) and other deep overflows. A second feature is the mixing between the winter and summer water (detailed below), a process that is consistent with strong downslope flow, supercritical conditions, hydraulic jumps and such. This behavior raises the possibility that hydraulic effects, and possibly hydraulic control, might be active in Herald Canyon, and that hydraulic models might be of some use in interpreting our observations. Pickart et al. (2005) have made the case that the flow of Pacific winter water through Barrow Canyon is subject to hydraulic control. The presence of hydraulic control, which acts to constrain the volume flux of the overflow, would impact the draining timescale of the upstream reservoir of dense fluid, in this case the winter water on the Chukchi Shelf. The most likely location for a control in Herald Canyon is Section 3, or its vicinity, where there is a sill (appearing in the IBCAO chart of Fig. 2A as well as in the measured topography of Fig. 6) and where the canyon is at its narrowest.

4.1. Are hydraulic processes relevant?

Rotating hydraulic theory has been developed around idealized models of sill flows, usually with a single active layer and with simplified canyon or strait geometry. The current state of the art is not equipped to handle the complex Herald Canyon flow, with its different water masses, frontal boundaries, and counter flow. While constructing a model that contains such complications is beyond the scope of this paper, we can estimate whether hydraulic effects are in fact relevant in the canyon. In particular, we can determine if the velocities are large enough for

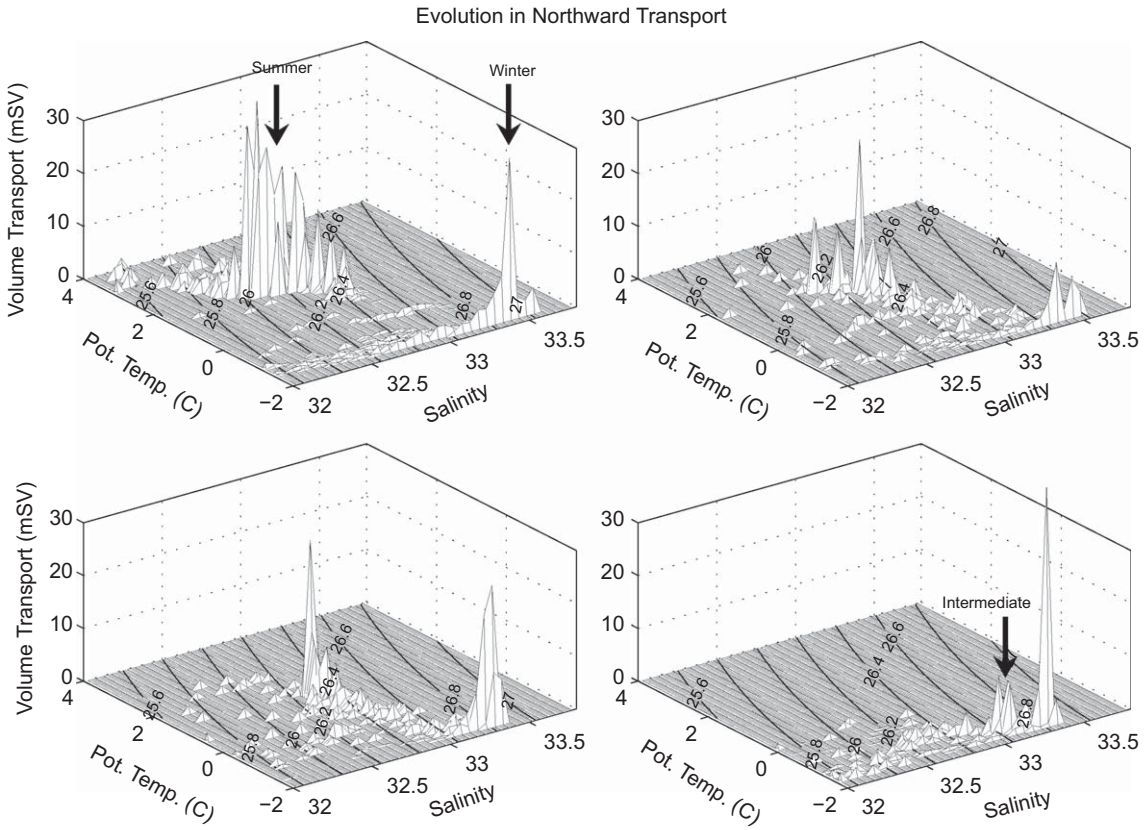

Fig. 7. Volume transport in milli-Sverdrups (mSv) as a function of potential temperature and salinity for the four transects. The three transport modes are marked by the arrows.

hydraulically critical flow (and corresponding subcritical-to-supercritical transitions) to occur. In a one-layer, non-rotating system, this would depend on the value of the internal Froude number, with values of order unity or greater indicating fluid velocities sufficiently large to arrest an internal wave that attempts to propagate upstream. For the present case, the stratification is closer to a three-layer system consisting of the winter water, summer water, and the near-surface water. We focus on Section 3 located near the sill (Fig. 3A), and in particular on the region of strongest flow on the eastern side of the canyon (from approximately 5 to 25 km, see Fig. 3D). The three density layers are chosen to be: the surface to $\sigma_\theta = 25.6$; 25.6–26.7; and 26.7 to the bottom. These choices are motivated by the hydrographic section of Fig. 2D (i.e. the surface water, summer water, and cold winter water).

There is no simply-defined Froude number for this scenario, so we instead turn to the critical condition for a three-layer system defined as such and determine whether the observed core velocities are reasonably close to criticality. The most appropriate condition is one recently derived by Pratt (2008), which extends Smeed's (2000) condition for critical flow by allowing cross-channel velocity variations within each layer. The criterion is

$$\tilde{F}_1^2 + \left(\frac{1-r}{r} + \frac{w_3}{w_2}\right)\tilde{F}_2^2 + \tilde{F}_3^2 - \frac{w_3}{w_2}\tilde{F}_1^2\,\tilde{F}_3^2 - \tilde{F}_1^2\,\tilde{F}_3^2\,\frac{1-r}{r}\tilde{F}_2^2\,\tilde{F}_3^2 = 1, \tag{4.1}$$

where ρ_n is the density of layer n ($n = 1$, 2, or 3, with 1 denoting the top layer), $r = (\rho_2 - \rho_1/\rho_3 - \rho_1)$ and

$$\tilde{F}_1^2 = \left(\frac{1}{w_2}\int_{x_{1L}}^{x_{1R}} \frac{g'_{21}D_1}{V_1^2}\,dx_1\right)^{-1},$$

$$\tilde{F}_2^2 = \left(\frac{1}{w_2}\int_{x_{2L}}^{x_{2R}} \frac{g'_{21}D_2}{V_2^2}\,dx_2\right)^{-1},$$

$$\tilde{F}_3^2 = \left(\frac{1}{w_3}\int_{x_{3L}}^{x_{3R}} \frac{g'_{21}D_3}{V_3^2}\,dx_3\right)^{-1}. \tag{4.2}$$

The parameter w_n is the lateral extent of layer n (x_{nL}–x_{nR}), $V_n(x_n)$ and $D_n(x_n)$ are the layer depths and velocities, and x is the cross-stream coordinate. The reduced gravities are $g'_{ij} = g\,(\rho_i - \rho_j)/\rho_o$, where ρ_o is the average density of the three layers. Note that $\tilde{F}_1^2$, $\tilde{F}_2^2$ and $\tilde{F}_3^2$ can be interpreted as generalized versions of layer Froude numbers. Eq. (4.1) describes a two-leafed surface that exists in the three-dimensional space ($\tilde{F}_1^2$, (w_3/w_2),$\tilde{F}_2^1$, $\tilde{F}_3^2$), as shown in Fig. 8A. Critical states must lie on one of the leaves of this surface. The first leaf covers an area near the origin and has finite extent (see the left-hand portion of Fig. 8A), while the second leaf lies farther from the origin and is unbounded. Of greatest interest for the present case is the first leaf, which separates subcritical (non-controlled) flows near the origin, from flows that are supercritical with respect to one wave.[2] In a hydraulically controlled flow, we would expect the sill flow to lie reasonably close to this surface.

We estimated the values of $\tilde{F}_1^2$, $(w_3/w_2)\,\tilde{F}_2^2$ and $\tilde{F}_3^2$ based on the observed density and velocity distributions at Section 3, using the layer definitions noted above. The values of the generalized

[2] As shown by Sannino et al. (2009), the second surface separates flows that are supercritical with respect to one internal mode from flows that are supercritical with respect to two modes. The situation is complicated by the fact that that flows on either side can be unstable with respect to these modes. None of our estimates of the generalized Froude numbers approach this surface.

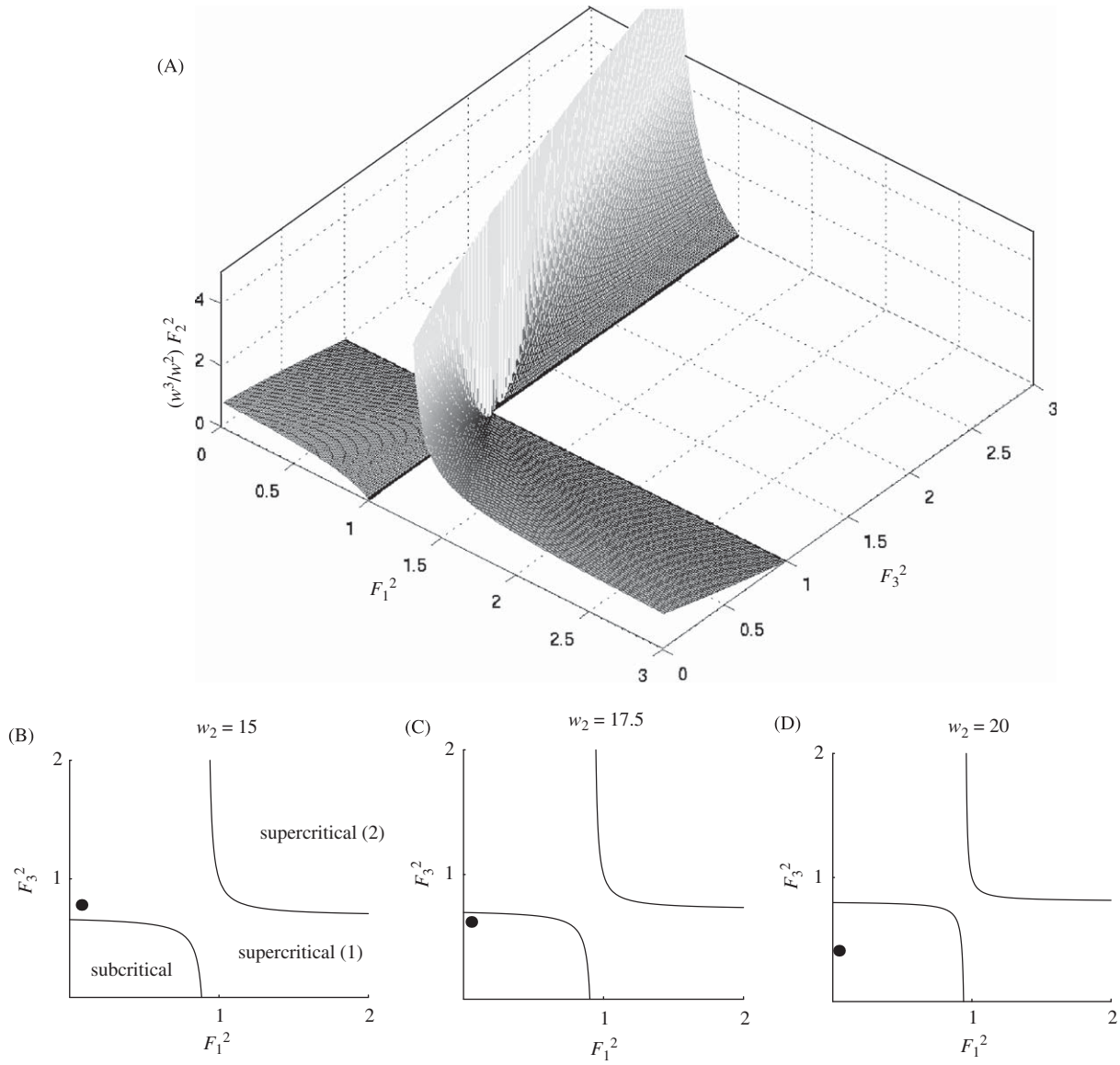

Fig. 8. (A) The surface defined by Eq. (4.1) for the setting $(1-r)w_3/rw_2 = 1/4$. The remaining frames show $(w_3/w_2)\,\tilde{F}_2^2 = constant$ slices through the surface for three approximations to the core of the Section 3 flow corresponding to three slightly different widths. The contours indicate where the critical surface in (A) cuts across this plane and the solid circle indicates the location of the observed state. (B) $r = 0.827$, $w_2 = 15.0$ km, $w_3 = 12.5$ km, $\tilde{F}_1^2 = 0.080$, $\tilde{F}_2^2 = 0.381$, and $\tilde{F}_3^2 = 0.789$; (C) $r = 0.825$, $w_2 = 17.5$ km, $w_3 = 15.0$ km, $\tilde{F}_1^2 = 0.056$, $\tilde{F}_2^2 = 0.328$, and $\tilde{F}_3^2 = 0.619$; (D) $r = 0.820$, $w_2 = 20.0$ km, $w_3 = 17.5$ km, $\tilde{F}_1^2 = 0.045$, $\tilde{F}_2^2 = 0.224$, and $\tilde{F}_3^2 = 0.418$.

Froude numbers depend on the lateral widths (w_2, w_3) over which the integrals in (4.2) are performed. The primary core of the flow at Section 3 (confined mostly to the eastern flank, including part of the winter water) occupies a width of 15–20 km (see Fig. 3D). We have chosen three pairs of (w_2, w_3) within that range as a basis for the calculation. The result for each case is best displayed on a two-dimensional slice through the first leaf of Fig. 8A, corresponding to $(w_3/w_2)\,\tilde{F}_2^2 = \text{constant}$ (see Fig. 8B–D). The critical surfaces cut through each of these planes along the two contours shown. If the calculated values of $(\tilde{F}_2^1, \tilde{F}_3^2)$, represented by the solid circles in Fig. 8B–D, lie inside the inner curve, the flow is subcritical. Values lying between the two curves are supercritical with respect to one of the wave modes of the three-layer system. As seen in the figure, the data points (solid circles in Fig. 8B–D) lie close to the inner critical curve for two of the cases shown, and somewhat below the curve for the final case (corresponding to the largest choice of the core width). Our conclusion, based on this, is that the flow at Section 3 lies reasonably close to a state of hydraulic criticality. At the very least, one can say that the flow velocities are of sufficient magnitude to arrest wave propagation.

4.2. Lock-exchange transport estimate

A crude, hydraulics-based estimate of the winter water transport through Herald Canyon can be made using ideas based on the classical, two-layer lock-exchange problem with rotation (see Section 5.8 in Pratt and Whitehead, 2008). This approach is motivated by the fact that wintertime winds in the area are generally from the northeast, which would tend to keep the winter water piled up in the Chukchi Sea. Relaxation of the winds in spring and summer would then allow the dense water to drain through Herald and Barrow Canyons. This idea is consistent with the observation that the coldest winter water appears downstream of Barrow Canyon in spring and summer after the winds have weakened (Pickart et al., 2005; Spall et al., 2008). In a

simplified framework, the release of dense water could be imagined to result from the removal of a barrier upstream of both canyons. The steady outflow that develops is similar in some respects to the dense flow in a lock exchange where two resting, homogeneous water masses of different density, contained in a channel and separated by a vertical barrier, are released.

In the lock exchange problem, removal of the barrier sets the two layers in motion in opposite directions, progressing above and below each other. Rotation causes each layer to turn to its respective right, and the interface subsequently develops a cross-stream tilt. When the channel is wider than about 3/2 the Rossby radius of deformation (which is the case in Herald Canyon), the interface detaches from the sidewalls of the channel and contacts the bottom and surface. In this limit the volume flux is given by $Q_w = Cg'D^2/f$, where g' is the reduced gravity, D is the depth of the channel, f is the Coriolis parameter, and C is a constant of proportionality. Several approaches have been used to estimate the quantity C. A value of $C = 0.208$ is predicted using an energy conservation argument (Hunkins and Whitehead, 1992), whereas $C = 0.176$ is predicted under the assumption that the flow at the position of the barrier becomes hydraulically critical (Rabe et al., 2007). Laboratory experiments by both groups, and by Dalziel (1988), produce values in the range 0.1–0.2.

This idealized framework can be used to form an analog of the Herald Canyon winter water outflow. For the dense layer we take $\sigma_\theta = 26.8\,\mathrm{kg\,m^{-3}}$, based on our RUSALCA measurements (see Fig. 2). To estimate the density of the ambient Arctic water (that is, the water on the other side of the lock), we used a hydrographic section occupied across the shelfbreak to the east of Herald Canyon (at 166°W, not shown). This section was occupied in July 2002, presumably soon after the dense water emanating from Herald Canyon reached this location. The section contained Pacific winter water on the outer shelf and shelfbreak, with comparable T/S characteristics to the winter water observed during RUSALCA. According to the numerical models discussed above, the winter water at 166°W likely originated from Herald Canyon (see also Section 6 below). The density of the ambient Arctic water was calculated by averaging over the depth range 0–60 m (mean depth at the Herald Canyon sill) for data seaward of the winter water at 166°W. The average value so computed was $\sigma_\theta = 24.7\,\mathrm{kg\,m^{-3}}$, resulting in $g' = 0.02\,\mathrm{m\,s^{-2}}$. With $f = 1.4\times10^{-4}\,\mathrm{s^{-1}}$ and $D = 60\,\mathrm{m}$, this gives $Q_w = 0.11$ Sv for the energy balance approach, and $Q_w = 0.09$ Sv when using the criticality assumption. These transport values are consistent with the observed northward volume flux of winter water from the RUSALCA survey (0.08 ± 0.026 Sv), and the non-winter water up-canyon transport on the western flank (0.077 ± 0.021 Sv, which is the average for Sections 2–4 since there was no up-canyon flow at Section 1). Therefore, the observed volume fluxes are consistent with the notion of a sudden release of dense water from the Chukchi Sea subject to hydraulic control. A strong caveat is that the model estimate ignores the dynamics of the summer water outflow.

4.3. Observational considerations

Additional evidence for hydraulic activity in Herald Canyon arises from inspection of a vertical section constructed along the length of the canyon (Fig. 9). The stations comprising the section are shown in Fig. 6A, situated along the core of the winter water. Within the dense layer, which corresponds roughly to the magenta shading in Fig. 9A, the deepest isopycnals ground as the water flows northward through the canyon. However, this trend reverses downstream of Section 3 near the mouth of the canyon, where the isopycnals lift off the bottom. This region corresponds to the increase in layer thickness in Figs. 6C and 2E. Interestingly, some of the properties of the layer show a deep tongue emanating from offshore in this region. For example, note the plume in turbidity near 60 m at station 74 in Fig. 9B. The tongue is present in other properties, including fluorescence, oxygen, and buoyancy frequency. The general pattern of density and tracers in this region is consistent with the "roller" region of an internal hydraulic jump, as described by Wilkinson and Wood (1971). The roller is a vertical, counterclockwise eddy that exists in a region where the bottom layer thickness increases rapidly in the downstream direction. The up-channel velocity at the top of the roller could produce a tracer tongue of the type observed. However, this interpretation is subject to caveats, one being that the present system experiences rotation not considered in the Wilkinson and Wood (1971) experiments.

Another possible consequence of the high velocities and strong shears in hydraulically driven flows is mixing. Most vertical overturning and mixing occurs as the result of shear instabilities and near-bottom turbulence, though additional mixing might occur in a hydraulic jump. There is evidence of mixing downstream of the sill in Herald Canyon. First, the distribution of Richardson number at Section 3 shows values smaller than one, both within the central portion of the dense layer as well as near the eastern edge of the layer, i.e. at the interface between the winter water and summer water (Fig. 10A). This suggests that vertical mixing may be active. Second, it is in this latter region where the new transport mode is established as the flow reaches Section 4. The inference then is that the creation of the transport mode is a consequence of this mixing. However, while such a scenario is plausible, there is more to the story than simple vertical overturning. This is because a mixture of the winter water and summer water in the vicinity of the interface (near the eastern edge of the dense plume) cannot fully account for the T/S characteristics of the intermediate transport mode. In order to create the mode, it is necessary to include a contribution from the western side of the dense plume as well (i.e. some colder, fresher water).

This is demonstrated as follows. If we construct a laterally averaged vertical profile of temperature and salinity for the eastern part of the plume (extending vertically from the winter water into the summer water), then vertically mix this, it does not match the properties of the intermediate transport mode of Section 4. However, if we expand the lateral average to include the entire portion of the plume that is flowing northward, the T/S of the resulting vertical mixture exactly matches that of the new transport mode. This suggests that water within the dense layer must be transported toward the eastern flank of the canyon in order to participate in the mixing. How can this happen? There are two contributing possibilities. The first is simply due to the fact that the entire dense layer progresses onto the eastern flank as the water flows northward (i.e. the transposition of the winter water discussed above). Additionally, there may be a cross-stream circulation within the layer that contributes to the eastward movement, as discussed next.

4.4. Role of the bottom boundary layer

Previous work on mid-latitude jets over sloping topography has demonstrated the importance of the bottom boundary layer (BBL) in dictating the behavior and structure of both the primary (alongstream) and secondary (cross-stream) flow patterns. For example, BBL dynamics are believed to contribute to the formation of shelfbreak fronts (Gawarkiewicz and Chapman, 1992), as well as the trapping of frontal jets to the bathymetry (Chapman and Lentz, 1994). Numerous studies have also demonstrated that the cross-stream flow within the bottom Ekman layer

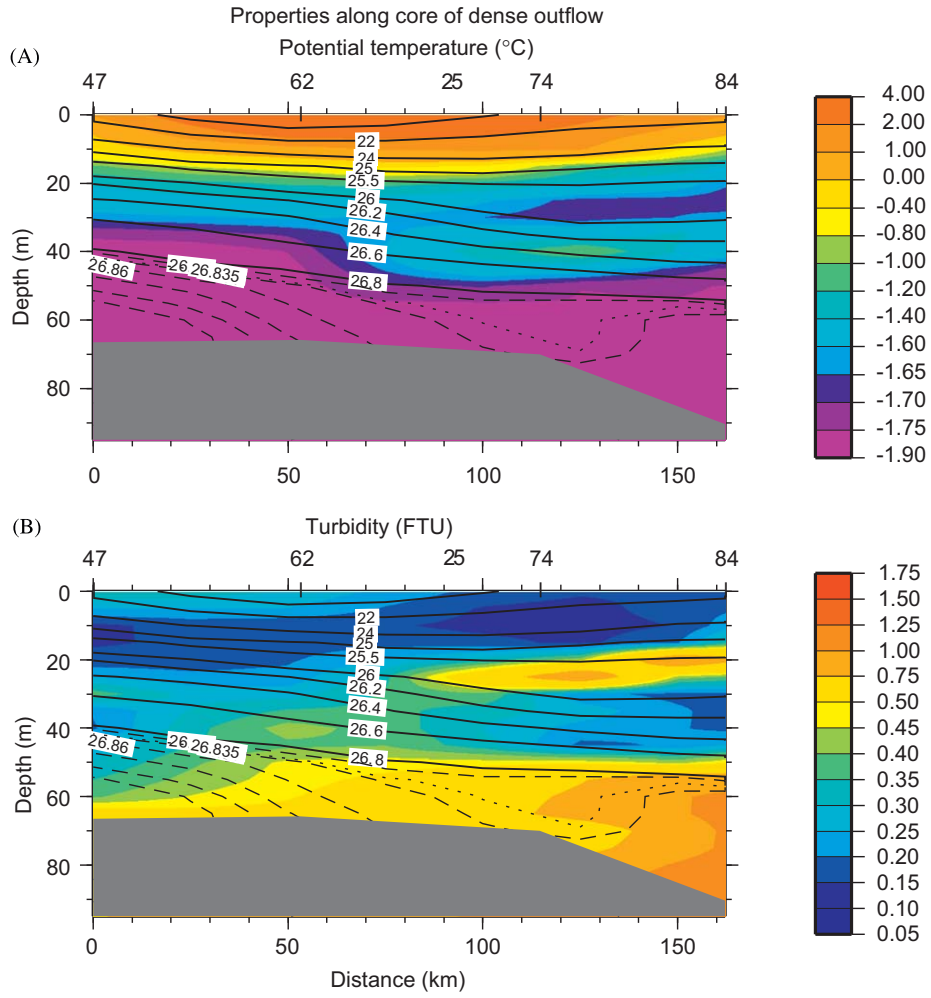

Fig. 9. Vertical sections along the core of the Herald Canyon dense outflow, constructed from the stations marked in Fig. 6. (A) Potential temperature (color), (B) Turbidity (color) overlain by potential density (contours, kg m^{-3}). Station numbers are indicated along the top. (For interpretation of the references to color in this figure legend, the reader is referred to the web version of this article.)

can, under certain circumstances, leave the bottom and progress along interior density surfaces. This process is known as bottom boundary layer detachment, and it was first investigated in the modeling study of Gawarkiewicz and Chapman (1992). An important consequence of BBL detachment is that nutrients, as well as other materials, can get pumped from the benthic layer into the interior of the water column. This has been observed in the shelfbreak jet of the Middle Atlantic Bight (e.g. Barth et al., 1998; Houghton and Visbeck, 1998; Pickart, 2000; Gawarkiewicz et al., 2009). One might expect that such dynamics would be at work in high latitude jets as well, and our survey provides evidence that BBL detachment occurs in Herald Canyon.

Using two different tracers, Pickart (2000) demonstrated that bottom boundary layer detachment occurred near the core of the middle Atlantic Bight shelfbreak jet, where there is convergence in the cross-slope bottom Ekman layer transport (see Fig. 17 of Pickart, 2000). At Section 3 (Fig. 3D), there is the northward jet of summer water on the eastern flank of the canyon, and a weaker up-canyon flow on the western flank. Using the LADCP velocities measured along this section, we computed the Ekman pumping based on the convergence of the near-bottom flow. In particular, the vertical velocity at the bottom was estimated by

$$w_{bot} = \left(\frac{\delta_E}{2}\right)\frac{d\overline{u}}{dx} \qquad (4.4.1)$$

where $\overline{u(x)}$ is the alongstream velocity averaged over the bottom 10 m of the section, x is the cross-stream coordinate, $\delta_E = (2\nu/f)^{1/2}$ is the Ekman depth, and ν is the vertical viscosity. Following Pickart (2000), a value of 1 cm^2 s^{-1} was used for the vertical viscosity. The cross-stream distribution of w_{bot} computed as such is shown in Fig. 10B. One sees that there are three regions of enhanced convergence in the BBL (i.e. positive peaks in w_{bot}): two narrow peaks centered at $x = 5$ and 50 km, and a third broader peak with maximum vertical velocity near $x = 35$–40 km (see the arrows in Fig. 10B). The first two features are analogous to the Ekman pumping analyzed by Pickart (2000) in the middle Atlantic Bight, that is, convergence in the BBL associated with an along-stream jet (in this case the down-canyon and up-canyon jets). The central peak is strongest in the region where the alongstream flow changes sign between southward and northward (meaning convergence due to oppositely directed flow in the BBL). The magnitude of the Ekman pumping in Fig. 10B is similar to that found by Pickart (2000) for the middle Atlantic Bight shelfbreak jet.

In light of Fig. 10B, there are three regions where one might expect to see detachment of the BBL in Herald Canyon. There is evidence from different tracers that this is indeed the case. Fig. 10C shows the cross-stream distribution of turbidity. There are two pronounced plumes of high turbidity emanating from the bottom near the location of the two narrow peaks in w_{bot}. These are highlighted by the eastern- and western-most arrows in Fig. 10C. (The slight discrepancy between the location of the

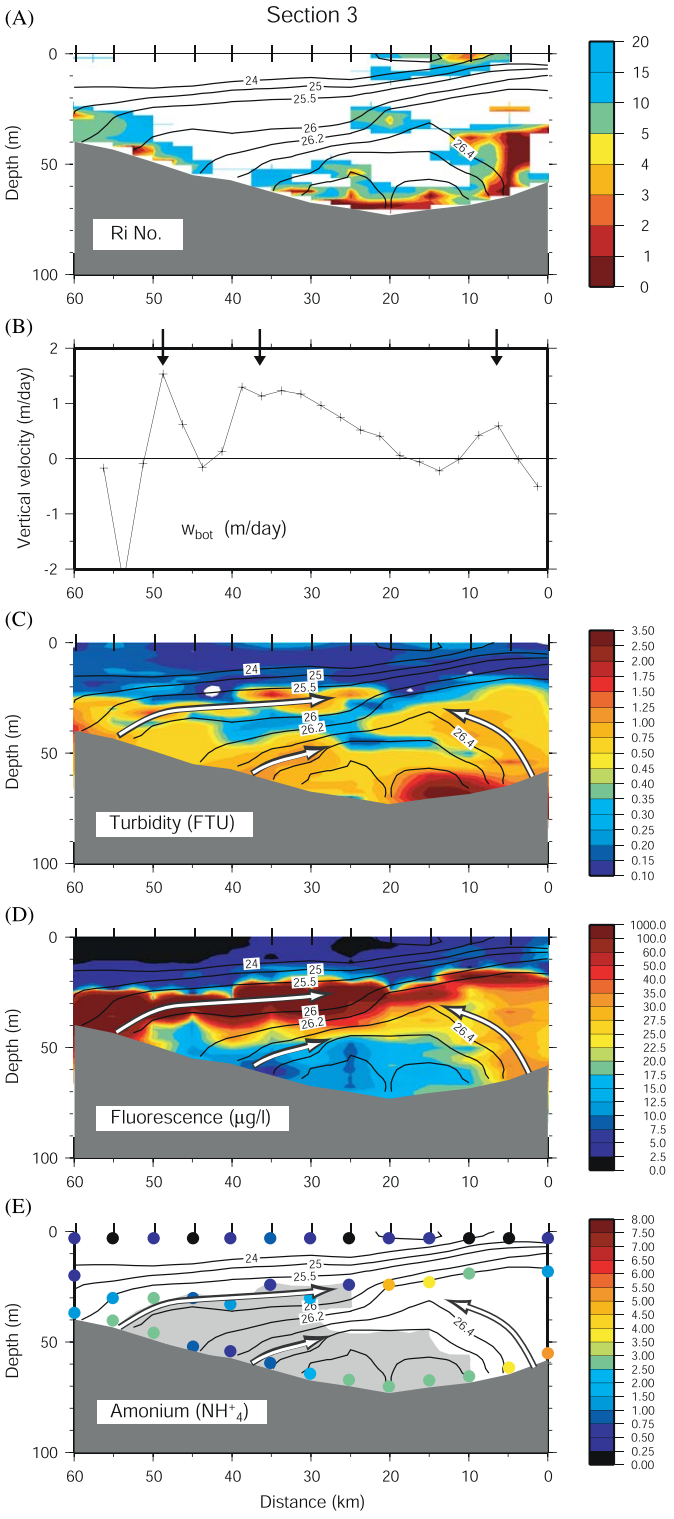

Fig. 10. Properties at Section 3. (A) Richardson number $= (N/u_z)^2$, where u_z is the vertical derivative of along-canyon velocity (color), overlain by potential density (contours, kg m^{-1}). Station locations are indicated along the top. (B) Cross-stream distribution of w_{bot}. The black arrows denote the three extrema of upward velocity. (C) Turbidity (color) overlain by potential density (contours). The arrows denote likely regions of bottom boundary layer detachment (see text). (D) Same as (C) for fluorescence (color). (E) Same as (C) for NH_4^+ (colored circles). The gray shading denotes the winter water, as in Fig. 5. (For interpretation of the references to color in this figure legend, the reader is referred to the web version of this article.)

vertical velocity peaks and the location where the plumes emanate from the bottom may be due to synopticity, since the velocity field is an instantaneous snapshot while the turbidity plumes represent a time average.) Consider first the eastern-most plume corresponding to the northward jet of summer water. Fig. 10D shows that this feature coincides with a tongue of high fluorescence as well, which in turn implies that phytoplankton from the spring bloom had likely settled to the bottom (as discussed earlier) and is being re-suspended via the BBL pumping mechanism. An interesting facet of this is implied by the distribution of ammonium (Fig. 10E). Once chlorophyll reaches the bottom it is decomposed by bacteria, releasing ammonium into the pore water. Hence, a detached BBL plume in an area where phytoplankton has settled should be characterized by elevated values of ammonium. This is indeed the case as seen in Fig. 10E (the spatial resolution of the bottles is limited).

Consider next the western-most turbidity plume in Fig. 10C, associated with the up-canyon jet. It shows similar features to the eastern plume, with elevated fluorescence (chlorophyll) and enhanced concentrations of ammonium. The particularly high values of fluorescence may call into question the notion that the fluorescence plume actually originates from the bottom, since sinking phytoplankton from the surface could account for some aspects of the feature. While this may be partly the case, the distribution of temperature indicates that BBL detachment was taking place as well. To wit, note that the plume is also characterized by a tongue of cold water (indicated by the gray shading in Fig. 10E). This is in contrast to the warm water of the eastern-most plume. The impact of these two opposing secondary flows (i.e. the eastern- and western-most arrows in Fig. 10C, D) can be seen by considering the progression of temperature through the canyon in Fig. 2. Note that the temperature front separating the winter and summer water becomes progressively more contorted as the water flows northward. In particular, one sees the interleaving of the warm and cold plumes, which is quite pronounced by Section 3. By the time the flow reaches Section 4, a complete exchange of these two water masses has occurred. In particular, Chukchi summer water ($\sigma_\theta = 26$–26.4) is found on the western flank of the canyon (between 25 and 45 m), while, at a slightly lower density ($\sigma_\theta = 25.5$–26), winter water resides on the eastern flank (between 5 and 25 m). This exchange seems to have been driven by the secondary circulation associated with BBL detachment, suggesting that such dynamics are important to the evolution of the flow.

Finally, the third turbidity plume in Fig. 10C extends from the region where the alongstream velocity changes sign from northward to southward, which corresponds to the maximum in w_{bot} near $x = 35$–40 km. (Note that the positive vertical velocities east of $x = 30$ km, on the shoulder of the broad peak, will not result in BBL detachment because this is within the densest portion of the winter water where the density surfaces in question are confined to the near-bottom layer.) The T/S characteristics of the water in this plume are precisely what is needed as the additional component to create the intermediate transport mode observed at Section 4 (as discussed above). The direction of flow in this detached layer, indicated by the third arrow in Fig. 10C–E, will bring the water toward the region where the vertical mixing is thought to be occurring. While we are not suggesting that the BBL detachment is dynamically linked to the hydraulic activity, it appears that the detached plume influences the final water mass characteristics of the new modal product emerging from Herald Canyon.

5. Origin of the winter water

As discussed in the introduction, the northward-flowing water that enters Herald Canyon on its eastern flank is believed to be part

of a direct route from Bering Strait. In the winter and spring this is winter-transformed water, and during the summer and fall it is summertime Bering Sea Water (Woodgate et al., 2005). During our August survey, it is likely that the jet of summer water on the eastern flank (Figs. 2 and 3) was part of this pathway. This idea is consistent with the hydrographic measurements taken in the southern/central Chukchi Sea during the RUSALCA survey. In particular, the CTD section from the Siberian coast to Cape Lisburne, Alaska (see Fig. 1 for the location of the stations) showed summertime Bering Sea Water over the western half of the section. What was the origin of the dense water entering the western side of Herald Canyon? We believe that it is not simply the result of an advective pathway from Bering Strait, and that it involves the existence of a reservoir of winter water in the area southeast of Wrangel Island. We now offer some clues as to how this reservoir might be formed and how it might be feeding the canyon.

5.1. *Dense water reservoir: role of the Wrangel Island polynya*

During winter and early spring, the whole of the Chukchi Sea is filled with winter water (Coachman et al., 1975), including both sides of Herald Canyon (Woodgate et al., 2005). The source of the winter water is a combination of inflow through Bering Strait (remote source) as well as brine-driven convection in the Chukchi Sea as the ice forms (local source). Although the pack-ice typically covers the sea by December, this does not mean that local convection ceases entirely. It is likely that the shifting/cracking of the ice, with subsequent re-freezing, provides a significant brine source throughout the winter (e.g. Cavalieri and Martin, 1994). This suggests that there are other factors, besides advection from Bering Strait, involved in forming the pool of winter water that supplies Herald Canyon in late-summer. One obvious candidate is the major polynya that opens up regularly in the vicinity of Wrangel Island (Cavalieri and Martin, 1994; Winsor and Björk, 2000).

To investigate this we analyzed the AMSR-E satellite ice concentration data for the winter preceding the RUSALCA survey (October 2003 to May 2004). During this winter, freeze-up occurred in the western Chukchi Sea in late-November. We tabulated the number of days, subsequent to freeze up, that the ice concentration was less than 65% in the vicinity of Wrangel Island and Herald Canyon. The results, displayed in Fig. 11A, indicate that regional polynyas opened up around the island, most prevalently off the western coast where there was reduced ice-cover on the order of 40–50 days between December and May. A time-series of the average ice concentration of the polynyas on the western side of the island (within the red box of Fig. 11A) reveals that there was a burst of polynya activity in the first part of winter (December–January), with some additional events in late-March through mid-April (Fig. 11B). In total there were 16 events of varying duration (the event starting in early May likely merged with the occurrence of melt-back later in the month).

Brine-driven convection within Arctic coastal polynyas is believed to be a significant source of dense water contributing to the ventilation of the cold halocline. Cavalieri and Martin (1994) estimated that the net transport from all of the polynyas is 0.7–1.2 Sv, while Winsor and Björk (2000) calculated a value significantly less than this (0.2 Sv). There are three regions in the Chukchi Sea where polynyas tend to form: adjacent to the eastern boundary of the sea between Cape Lisburne and Barrow; along the coast of Siberia; and in the vicinity of Wrangel Island. The first of these appears to be the most significant source of dense water; Cavalieri and Martin (1994) state that it is the second largest

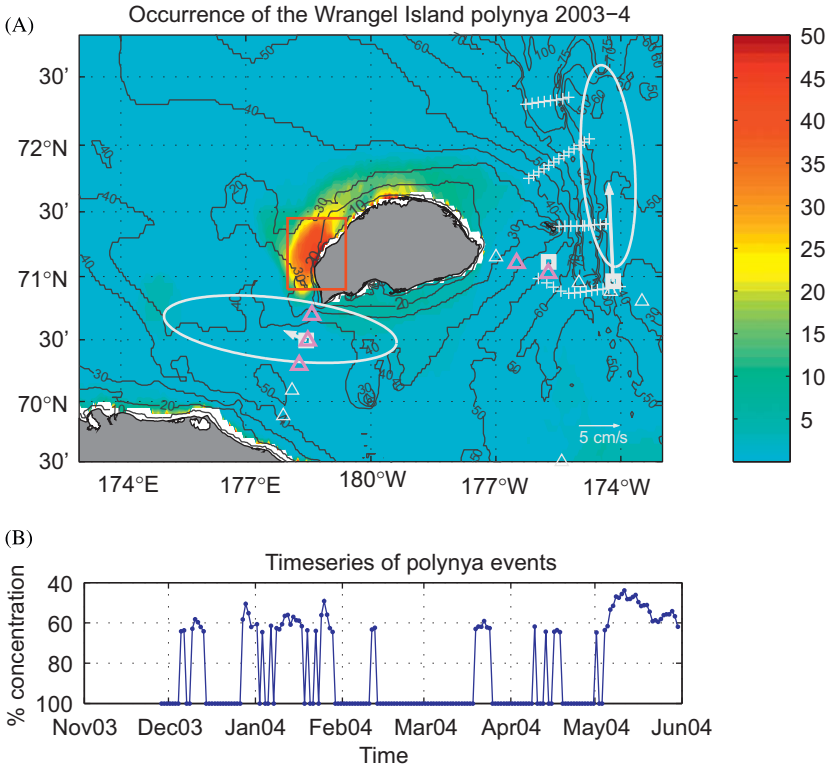

Fig. 11. The Wrangel Island polynya in winter 2003–2004. (A) Number of days, after freeze up occurs, that the pack-ice concentration is $<65\%$ (color). Also shown are the 2004 RUSALCA Herald Canyon stations (white +'s), the 1991 CTD stations (triangles, where violet indicates that winter water was present at the station), the locations of the 1990–1991 current meter moorings (white squares), and the mean current vectors and standard deviation ellipses at the two current meter sites with year-long records (see text for details). (B) Average pack-ice concentration of the polynyas within the red box in (A). (For interpretation of the references to color in this figure legend, the reader is referred to the web version of this article.)

source of polynya water in the Arctic. However, the Wrangel Island polynya is quite active as well. Using a polynya model driven by NCEP winds and air temperature over 39 winters, Winsor and Björk (2000) found that the Wrangel Island polynya typically opened up 30 times per winter. Furthermore, their model indicated that the final salinity of the dense water so produced was on average 36–37. It is likely that this estimate is too salty, based on nearby wintertime measurements (Woodgate et al., 2005), and because Winsor and Björk's (2000) model did not consider the dynamical response of the water column to brine-driven convection. As demonstrated by Winsor and Chapman (2002), the lateral buoyancy flux due to eddies tends to limit the increase in salinity as time progresses. Nonetheless, the studies of Cavalieri and Martin (1994) and Winsor and Björk (2000), together with the results displayed in Fig. 11, suggest that the region surrounding Wrangel Island represents a significant source of dense water to the western Chukchi Sea.

While winds are necessary to open up a polynya, Pease (1987) argued that the final area of open water formed is more sensitive to air temperature, since subsequent ice formation is limited when the air is warmer, and vice versa. The oceanographic model of Chapman (1999), however, suggests that the magnitude of dense water fluxed from a polynya is most strongly dependent on the winds. It is of interest then to consider the atmospheric conditions that led to the formation of the Wrangel Island polynya during the winter of 2003–2004 prior to our hydrographic survey. Inspection of the NCEP fields corresponding to the events in Fig. 11B revealed that there was a typical atmospheric pattern conducive for the formation of the polynya. Specifically, six out of the seven largest events were characterized by the presence of a low-pressure system in the vicinity of the Bering Sea.

The composite of these events shows a well defined minimum in sea-level pressure, which is due to the passage of Aleutian low-pressure systems (Fig. 12A). These systems develop during the fall and winter months (Overland and Hiester, 1980), and they tend to intensify south of the Alaskan Peninsula and Aleutian Island Arc. They generally weaken once they progress into the Bering Sea (Pickart et al., 2008). Nonetheless, a strong pressure gradient exists to the north of the composite low in Fig. 12A, due in part to the presence of the Siberian high. Accordingly, a band of strong easterly winds is present across the north end of the East Siberian and Chukchi Seas, with a maximum in the vicinity of Wrangel Island (Fig. 12B). These strong winds in turn open up the polynya adjacent to the island. The corresponding average air temperature near the island is between −5 and −10 °C (also from NCEP, not shown). Since Aleutian low-pressure systems are very common in fall and winter, this offers further support to the notion that the Wrangel Island polynya occurs regularly each year. It also suggests that, if more storms veer northward into the Bering Sea, the polynya activity will increase accordingly.

5.2. Circulation into the canyon

Once the winter water is formed, whether it be in the vicinity of Wrangel Island or elsewhere, what is the mechanism(s) by which it enters the western side of Herald Canyon? Here we consider three possible contributing factors (which may all be acting together to some degree): pressure head forcing associated with the dense water reservoir; wind forcing; and advection due to the Bering Strait inflow.

5.2.1. Dense water pressure head

A series of recent modeling studies (Chapman, 1999, 2000; Gawarkiewicz, 2000) have investigated the oceanographic response to brine-driven convection within polynyas. One of the fundamental aspects of the response is the development of small-scale eddies that flux the dense water away from the patch of open water. This leads to a steady state between the air-sea buoyancy flux and the lateral eddy flux, which limits the final density of the water mass product. In Gawarkiewicz's (2000) study, the eddies tended to coalesce in the presence of sloping topography, forming an along-slope gravity current. It might be expected then that the topography surrounding Wrangel Island would channel the dense

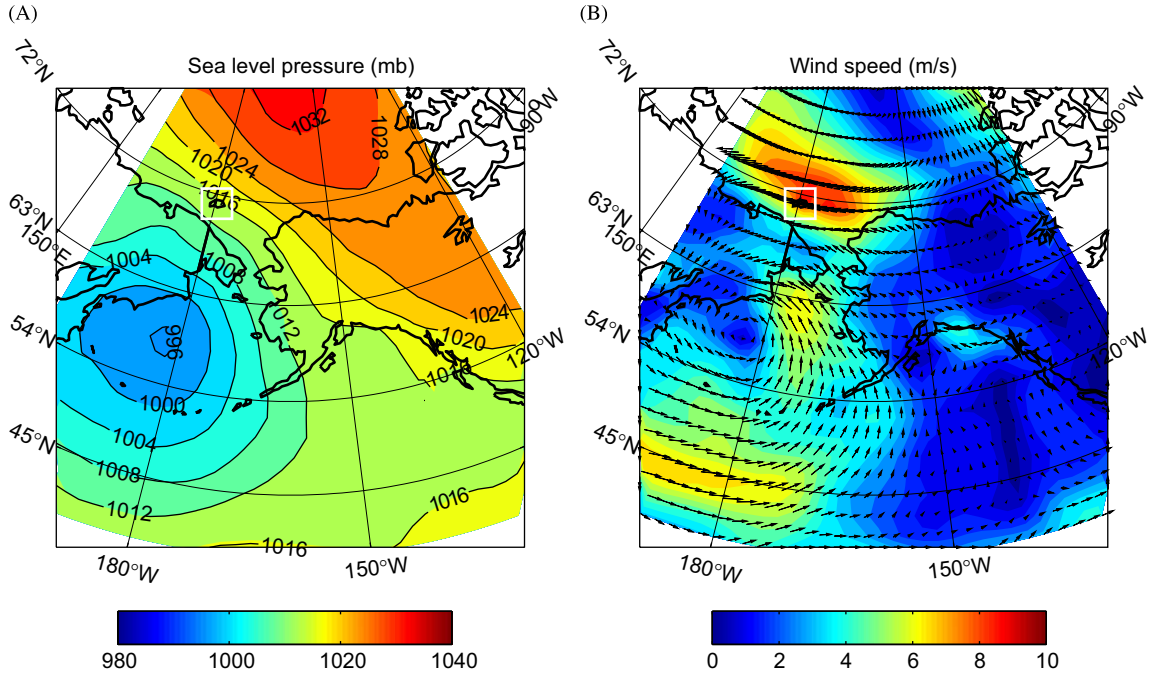

Fig. 12. Composite average of the meteorological conditions during the Wrangel Island polynya events in 2003–2004 (see text for details). (A) Sea-level pressure (color and contours). The location of Wrangel Island is marked by the white box. (B) 10 m wind speed (color) overlain by the wind vectors. (For interpretation of the references to color in this figure legend, the reader is referred to the web version of this article.)

polynya water in an anti-cyclonic sense around the island, since this is the direction of Kelvin wave propagation associated with geostrophic adjustment. Another reason to expect anti-cyclonic flow is that this is the sense of the tidally induced current according to Kowalik and Proshutinsky's (1993) model. Due to the presence of bottom friction, the dense water might also descend to somewhat deeper depths as it flows around the island. Hence, the plateau on the southern side of the island (note the southward excursion of the 40 and 50 m isobaths in Fig. 11A) would divert the water offshore to form a reservoir. The associated pressure head from this dense reservoir could then drive the winter water into Herald Canyon. Since melt-back of the pack-ice in this area occurs as late as May/June, this would insulate such a pool of water (in contrast to the area directly south and east of the canyon, which is subject to solar heating much sooner), allowing it to stay cold and dense while draining into the canyon during summer.

Clearly this scenario needs verification, presumably using a numerical model. While such an investigation is beyond the scope of the present study, data obtained from a field program in 1990–1991 sheds some light on this issue. From September 1990 to October 1991 three moorings were maintained in this area, two at the head of Herald Canyon (one on each side of the canyon), and one in Long Strait (marked by the white squares in Fig. 11A). Unfortunately, the current meter on the western side of the canyon failed after 3.5 months. The year-long mean vectors and standard deviation ellipses for the other two moorings are shown in Fig. 11A. On the eastern flank of Herald Canyon the mean flow is northward and strong, which is not surprising since this is along the pathway extending from Bering Strait. During most of the year the flow at this site was poleward, and during the summer months (May–September) the flow was nearly unidirectional (Fig. 13A). The time-series of Fig. 13A indicate that summer water began to arrive on the eastern flank in early July (note the increase in temperature and decrease in salinity), coincident with an increase in the flow speed.

The situation in Long Strait was very different. Here the mean velocity was quite weak in relation to the standard deviation, and the flow reversed direction often. During the summer, the flow alternated between predominantly northwestward (towards the East Siberian Sea) and southeastward (towards the Chukchi Sea, Fig. 13B). Furthermore, the water remained cold and salty; that is, winter water was present throughout the summer at the mooring site. During the deployment and recovery of the moorings, hydrographic sections were occupied across Long Strait and across the head of Herald Canyon (the latter section nearly coincident with our southern-most hydrographic line). In Fig. 11A the locations of the stations occupied in October 1991 are marked (white triangles), and those stations where winter water was present are highlighted (magenta triangles). One sees that winter water was present on the north side of Long Strait, and on the western flank of Herald Canyon. In light of this, together with the mooring results, it is tempting to conclude that, in summer, dense water in Long Strait periodically feeds into Herald Canyon during eastward flow bursts of the type seen in the Long Strait mooring record. This may indeed be part of the story, but the *T*/*S* time-series from the mooring on the western side of the canyon suggests that it is not the complete story.

Note in Fig. 13C that, during the summer months, winter water alone was observed on the western flank of the canyon as well. However, the water on this side of the canyon was saltier (and denser) than the water observed in Long Strait from June onward. This argues against a simple advective pathway from Long Strait to the western side of Herald Canyon. It also offers indirect evidence for the reservoir scenario outlined above. In particular, if the densest polynya water flows anti-cyclonically around Wrangel Island and diverts offshore south of the island (to the east of Long Strait) and into the canyon, then the salinity on the western flank of the canyon should be greater than that observed in Long Strait—which is indeed the case in Fig. 13.

5.2.2. *Wind forcing*

Until now, the discussion concerning the flow of winter water entering the western side Herald Canyon has ignored the role of the wind, which may be important (at least at times). As

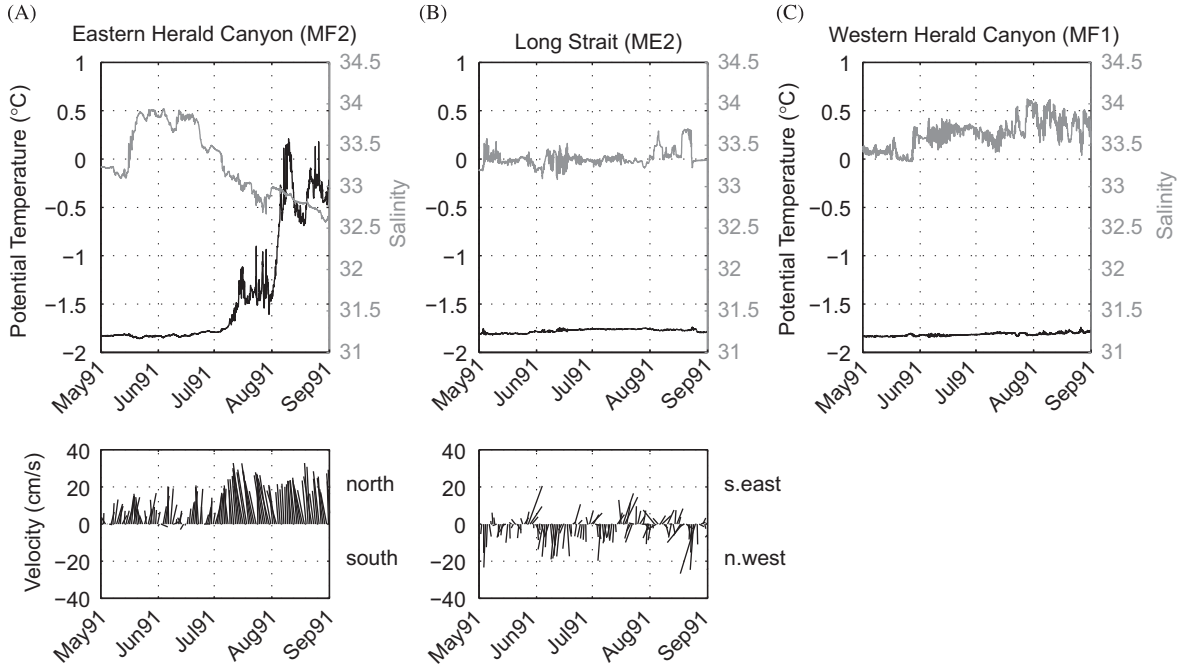

Fig. 13. Mooring time-series from May to Aug 1991 in (A) eastern Herald Canyon; (B) Long Strait; and (C) western Herald Canyon. See Fig. 11 for mooring positions. The top panels show the hourly potential temperature (black) and salinity (gray) records, and the bottom panels show the lowpassed, subsampled (once per day) current vectors. For the Long Strait velocity vectors, southeast is defined as 114°T. Note that there were no velocity data during this time period for the western Herald Canyon mooring.

mentioned in the introduction, strong southward flow into Barrow Canyon is commonly observed (e.g. Aagaard and Roach, 1990), driven by a variety of mechanisms, including northeasterly winds (e.g. Mountain, 1974). This up-canyon flow is usually accompanied by upwelling of warm and salty Atlantic water into the canyon. Coachman et al. (1975) speculated that a similar up-canyon flow occurred in Herald Canyon as well. However, Woodgate et al. (2005) found that the velocity record from the mooring on the canyon's eastern flank was not significantly correlated with the local wind field. (Interestingly, this was the only one of the 12 moorings deployed in the Chukchi Sea in 1990–1991 that was not correlated with the wind.) As seen in Fig. 13A, the flow was northward virtually the entire summer of 1991 on the eastern side of the canyon.

There were, however, a few significant up-canyon flow events during the remaining part of the year, most notably one in late September 1990 and one in early November 1990 (not shown). Despite the fact that, statistically, the flow was not correlated with the wind over the full year, inspection of the NCEP fields reveals that the two fall events noted above were associated with strong northerly winds (Fig. 14). The winds during the first event arose because of a large low-pressure system passing south of Bering Strait (Fig. 14A), while in the later event the winds were due to a strong ridge of high pressure associated with the Siberian high (Fig. 14B). Fortunately, the mooring located on the western flank of the canyon (see Fig. 11 for the location of the mooring) was still recording during the fall, and both of these wind events were observed to cause flow reversals on the western side of the canyon as well. The mooring in Long Strait also recorded enhanced flow during the latter period directed to the west out of the Chukchi Sea towards the East Siberian Sea. The peak of the flow observed in Long Strait lagged several days behind the southward flow in the canyon, and may have been due simply to mass continuity (i.e. the up-canyon flow had to go somewhere). However the westward flow in the strait was likely driven in part by the winds shifting out of the southeast a few days after the up-canyon flow event. These results indicate that, at times, local wind forcing can strongly impact the flow in this region. This in turn implies that the draining of the dense water into the western side of the canyon as described above may be occasionally disturbed (i.e. possibly halted by northerly winds, or possibly enhanced by southerly winds). We are unable to test this definitively because the current meter record on the canyon's western flank was so short. In any case, the winds before and during our August 2004 hydrographic survey were weak, so there was likely minimal wind-driven influence on the flow entering the western side of the canyon at that time.

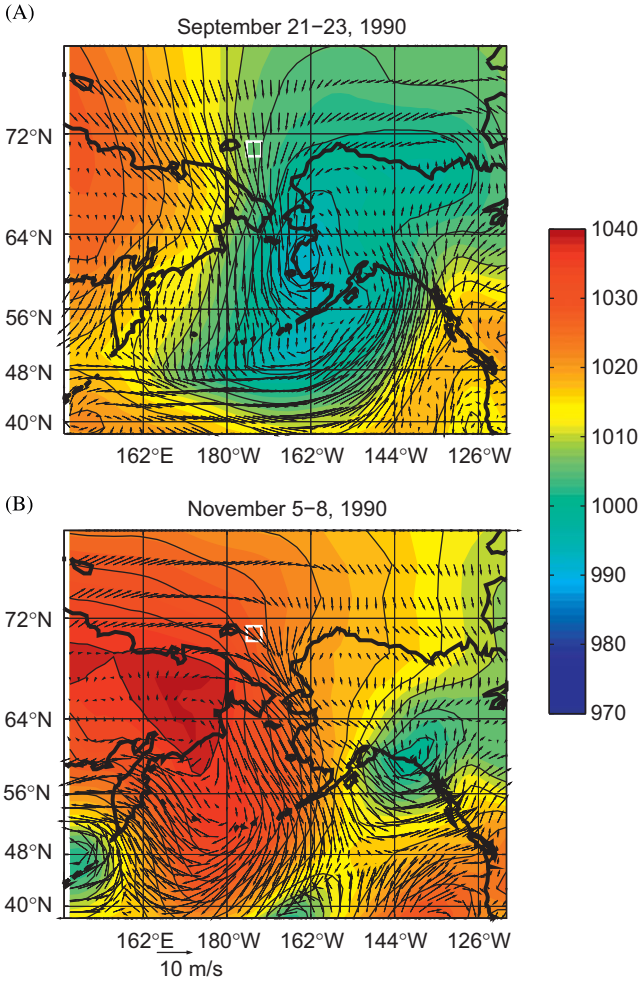

Fig. 14. Average meteorological conditions during the two strongest up-canyon flow events in 1990–1991, as measured by the eastern Herald Canyon mooring (MF2, denoted by the white box). Sea-level pressure (color, contours) is overlain by the 10 m wind vectors. (A) Average from 21 to 23 September, 1990. (B) Average from 5 to 8 November, 1990. (For interpretation of the references to color in this figure legend, the reader is referred to the web version of this article.)

5.2.3. *Role of Bering Strait inflow*

The final factor to be be considered regarding the summertime circulation of winter water into the western side of Herald Canyon is the remote influence of the Bering Strait inflow. As presented in Codispoti and Richards (1968), nutrient signatures in the East Siberian Sea are indicative of Pacific-origin water. Furthermore, the mean flow on the northern side of Long Strait is directed to the west (Fig. 11). Using this mooring record, Woodgate et al. (2005) estimated that 0.18 Sv (approximately 20% of the Bering Strait inflow) leaves the Chukchi Sea through the strait. It is likely then that the circulation south of Wrangel Island (i.e. the area where the dense water enters the western side of the canyon) can be forced remotely as well, via advection.

To investigate this we used the numerical model of Proshutinsky (1993). This is a pan-Arctic, two-dimensional, ice-ocean barotropic model with a horizontal resolution of approximately 14 km. The model has no thermodynamics, and the ice thickness is fixed corresponding to mean climatic conditions (see Proshutinsky and Johnson, 1997). The ice concentration is prescribed from observations obtained from the National Snow and Ice Data Center, and the ice dynamics includes internal ice forces as dictated by Rothrock (1975). The model uses realistic topography and is forced by NCEP winds and by a steady inflow through Bering Strait. For further details on the numerics of the model, including various applications, the reader is referred to Proshutinsky (1993), Kowalik and Proshutinsky (1994), and Proshutinsky and Johnson (1997).

The model has been run for the time period 1948–2007, and separate simulations carried out with and without winds. Here we focus on the time period of August, 2004. In particular, we averaged the model output over the week preceding the hydrographic survey in order to consider the manner in which the water was entering Herald Canyon. Keep in mind that the model is barotropic and hence cannot capture the dynamics associated with a pressure head driving winter water into the canyon from a reservoir. Instead, we use the model to investigate the role of the Bering Strait inflow. Fig. 15A shows the average flow field from 12 to 18 August, due to the combination of winds and inflow. Several interesting features are present. First, the flow entering the eastern side of the canyon emanates directly from Bering Strait along a fast pathway, as expected. Note that the

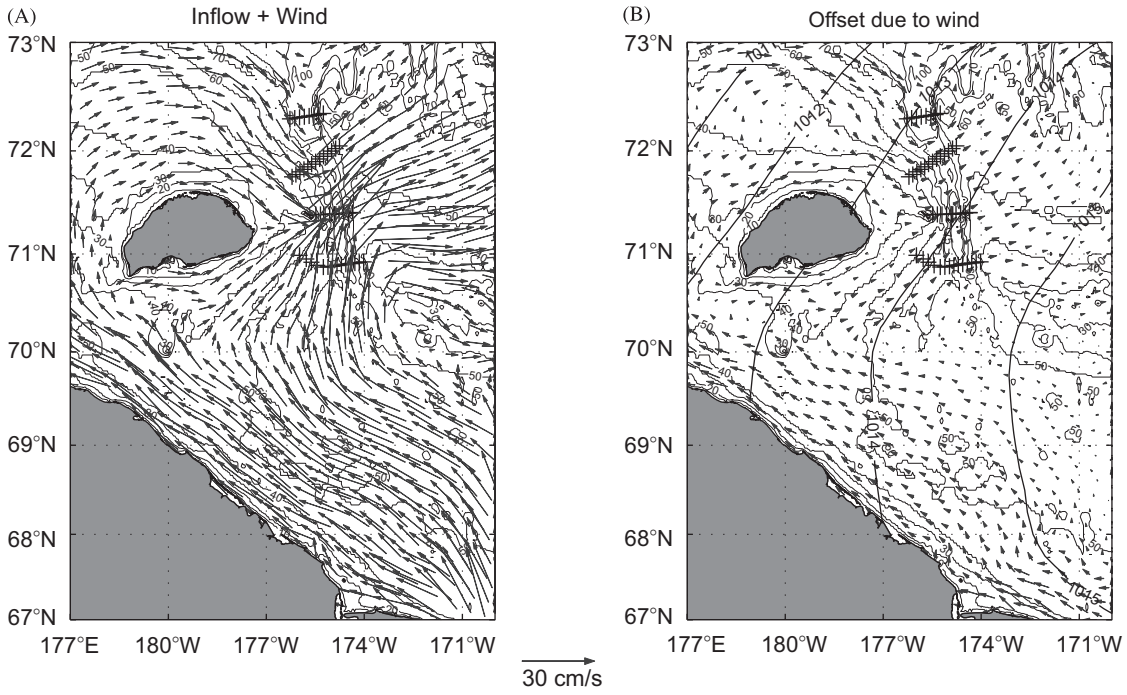

Fig. 15. Output from Proshutinsky's (1993) barotropic model averaged over the time period 12–18 August, 2004. (A) Flow vectors for the case when the model is forced by inflow from Bering Strait plus winds. Station positions of the RUSALCA hydrographic survey are indicated by the black crosses. (B) Residual flow due to the wind only (i.e. the case in (A) minus the no-wind case). The average sea-level pressure field is shown as well (contours in mb).

current vectors bend to the east around the north side of Herald Shoal, further supporting the idea that the warm water jet was diverted away from the mouth of the canyon, consistent with the northward reduction of summer water transport observed in our hydrographic survey. Second, the flow adjacent to Siberia is to the northwest extending into Long Strait. This is opposite to the direction of the East Siberian Coastal Current, a surface-trapped jet that has been observed in summer (Weingartner et al., 1999). While the model is unable to capture such a buoyancy-driven current, it is worth pointing out that the coastal current varies on interannual timescales and can be completely absent in a given summer (Weingartner et al., 1999). As seen in Fig. 15A, the model flow along Siberia forces a current in an anti-cyclonic sense around Wrangel Island. Finally, the water southeast of Wrangel Island is flowing into the western side of Herald Canyon. Fig. 15B shows the residual circulation due to the wind only. Not surprisingly it is weak, confirming our assumption that the flow measured during the hydrographic survey was not significantly impacted by the wind.

The barotropic model implies that there is a less direct and weaker pathway of water from Bering Strait to the western side of Herald Canyon (i.e. the flow is diverted to the area south of Wrangel Island where it slows down, before turning eastward again). This raises the possibility that the dense water entering the western flank of the canyon during our survey simply took this slower route, arriving at the same time as the summer water taking the faster route to the eastern side of the canyon. However, based on the evidence above, it is difficult to imagine that the dense water formed from the Wrangel Island polynya does not play a significant role. One possibility is that the polynya water may be partially advected by the ambient flow in Fig. 15A. The anti-cyclonic circulation north of Wrangel Island would bring polynya water towards the canyon (although, based on our hydrographic survey, it is unlikely that the flow enters the canyon near Section 2 as the model shows, but rather progresses farther around to the region southeast of the island). As seen in Fig. 15A, the flow in the area where the dense water reservoir likely exists is directed towards the western side of the canyon. The barotropic model suggests then that, even in the absence of a pressure head south of Wrangel Island, the ambient flow would tend to feed the polynya-origin winter water into the western side of Herald Canyon when the winds are weak.

6. Summary and discussion

Our results have revealed a previously unobserved summertime flow regime in Herald Canyon. At the time of the hydrographic survey, winter water entered the western side of the canyon and flowed northward alongside a strong jet of summer water on the eastern flank. As the dense water progressed down the canyon it switched to the eastern flank and underwent a sudden increase in layer thickness. Vertical mixing near the canyon mouth resulted in the formation of a new transport mode, which is intermediate to the winter and summer water masses. We have argued that the transposition and stretching of the dense water, its volume transport, and the mixing that occurs are all consistent with the occurrence of hydraulic activity within the canyon. The dense water feeding the canyon seems to originate from a reservoir of winter water located southeast of Wrangel Island. This pool of water is likely formed in part by polynya water emanating from the western side of the island during winter and circulating anti-cyclonically to the area south of Herald Canyon. The winter water presumably enters the western side of the canyon due to the pressure head of the reservoir, perhaps aided by advection of the ambient flow from Bering Strait. Because the Wrangel Island polynya forms on a regular basis and is driven by a commonly occurring wintertime atmospheric circulation pattern, we suspect that the scenario revealed by our 2004 hydrographic survey is typical of the summertime flow pattern in Herald Canyon under weak wind forcing.

An obvious next question to ask is, what is the fate of the Pacific water exiting Herald Canyon? Different scenarios have

been put forth in the literature regarding this issue. In the barotropic model of Winsor and Chapman (2004), when no wind is present, virtually all of the Pacific water exiting Herald Canyon turns to the right and flows eastward along the Chukchi shelfbreak. The same is true in the circulation model of Spall (2007) when the model is run without wind. The situation changes, however, when wind is present. In Winsor and Chapman's (2004) model the barotropic streamlines extend off the shelf into the interior basin for a pure easterly wind. Spall's (2007) study uses more realistic atmospheric forcing (daily NCEP fields for the year 2000) and has 12 levels in the vertical. When averaged over the year the wind is from the northeast, and a portion of the mean flow through Herald Canyon is diverted offshore. However, this offshore transport is confined primarily to the surface Ekman layer, which is only about 20 m thick. Hence, Spall's (2007) model implies that, with or without wind, the subsurface water masses leaving Herald Canyon should be channeled into an eastward-flowing boundary current along the edge of the Chukchi Sea.

An alternative scenario for the water exiting Herald Canyon has been put forth by Steele et al. (2004). Based on the distribution of summertime Bering Water in the interior Canadian Basin, they constructed a schematic flow pattern in which the summer water progresses northward from the canyon into the transpolar drift. While this scheme is at odds with the model results of Spall (2007), it does explain the offshore presence of the summer water (e.g. in the region of the Chukchi Borderlands). A definitive answer regarding the fate of the Herald Canyon outflow will require further measurements and detailed modeling. However, we can offer a few insights by comparing the results of our hydrographic survey to observations collected as part of the SBI program.

In September 2004 a hydrographic section was occupied across the Chukchi outer shelf and slope at 166°W, roughly 350 km to the east of Herald Canyon (Fig. 1). Based on the RUSALCA velocity measurements, the winter water exiting the canyon would have reached this location about the time the SBI section was occupied. As seen in Fig. 16, Pacific winter water was indeed present near the shelfbreak at 166°W, with similar *T*/*S* characteristics (Fig. 16A) and a similar nutrient signature (Fig. 16B) to the winter water flowing out of Herald Canyon. Vessel-mounted ADCP measurements were collected during the SBI cruise, and the section of alongstream velocity is shown in Fig. 16C. (These data were de-tided using the same procedure applied to the lowered ADCP data, as described in Section 2.1.) Interestingly, instead of showing an eastward-flowing shelfbreak jet, the vessel-mounted ADCP data revealed a westward-flowing surface-intensified current offshore of the shelfbreak, with eastward flow on the outer shelf. This scenario is reminiscent of a wind-driven flow reversal, as observed elsewhere on the Chukchi slope (Llinas et al. (2009)) and on the Beaufort slope (Nikolopoulos et al., 2009). Inspection of the NCEP fields reveals that northeasterly winds blew during the 5-day period prior to the occupation of the section, so the observed westward flow in the September 2004 166°W section is in fact not surprising.

There is increasing evidence that, when the winds are weak, the boundary current located along the edge of the Chukchi and Beaufort Seas flows to the east (Weingartner et al., 1998; Mathis et al., 2007; Nikolopoulos et al., 2009), consistent with the numerical models discussed above. Indeed, during the summer 2002 occupation of the 166°W SBI section the boundary current was flowing eastward under light winds. Hence, based on the similarity of the winter water observed exiting Herald Canyon to that seen in Fig. 16, it is logical to assume that the canyon outflow feeds the Chukchi shelfbreak jet. To investigate this more closely we compared the average *T*/*S* properties of the winter water between Herald Canyon and 166°W (Fig. 17). This indicates that,

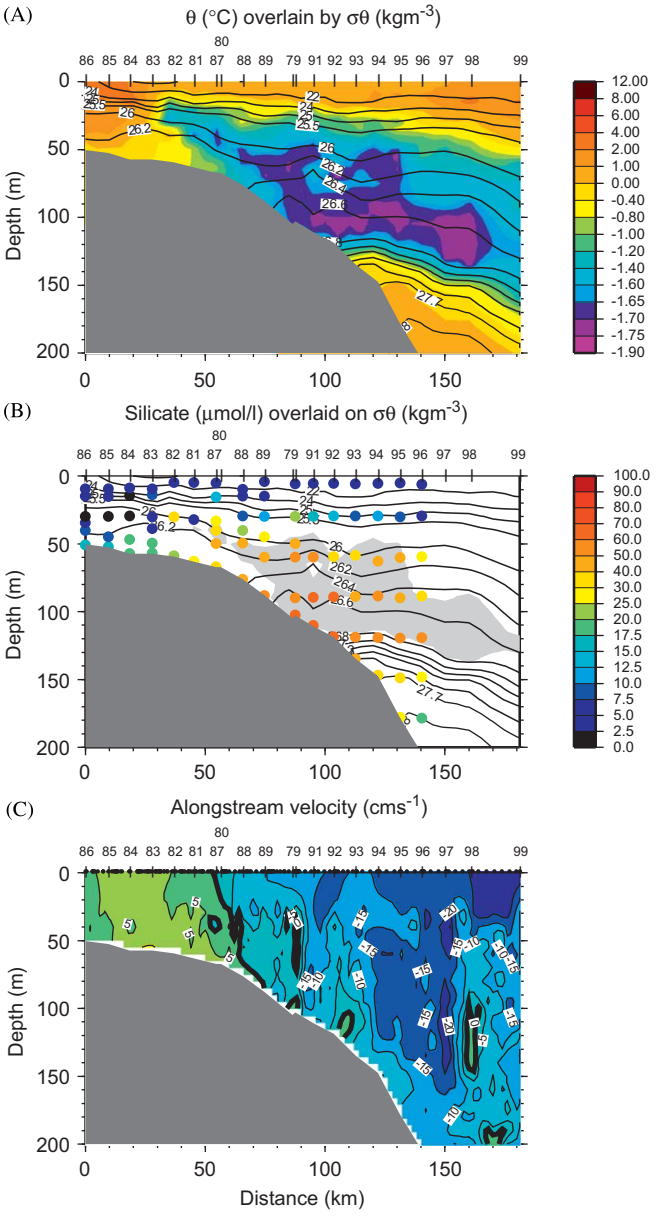

Fig. 16. Vertical sections across the Chukchi shelfbreak/slope at 166°W, occupied in September 2004. Station numbers are indicated along the top. (A) Potential temperature (color) overlain by potential density (contours). The color scale is the same as in Fig. 2 to facilitate comparison to Herald Canyon. (B) Silicate (colored circles) overlaid on potential density (contours). The gray shading denotes the winter water (potential temperature ≤ -1.6 °C). The presentation is the same as in Fig. 5 to facilitate comparison to Herald Canyon. (C) Alongstream velocity from the vessel-mounted ADCP. Positive contours are eastward. The lateral spacing of the ADCP measurements is indicated on the top (black circles). (For interpretation of the references to color in this figure legend, the reader is referred to the web version of this article.)

as the winter water flows down the canyon and into the shelfbreak jet, it becomes warmer and fresher (likely due to mixing with the ambient Arctic water). Fig. 17 also indicates that if any of this water is fluxed into the interior basin, it would ventilate the upper halocline, consistent with the results of Pickart (2004).

Finally, note in Fig. 16A that the stations on the outer shelf contain Chukchi Summer water in the layer adjacent to the bottom, similar to that found in Herald Canyon (Fig. 2). This is consistent with data collected previously during SBI on the Chukchi slope in early fall (R. Pickart, unpublished data). In light

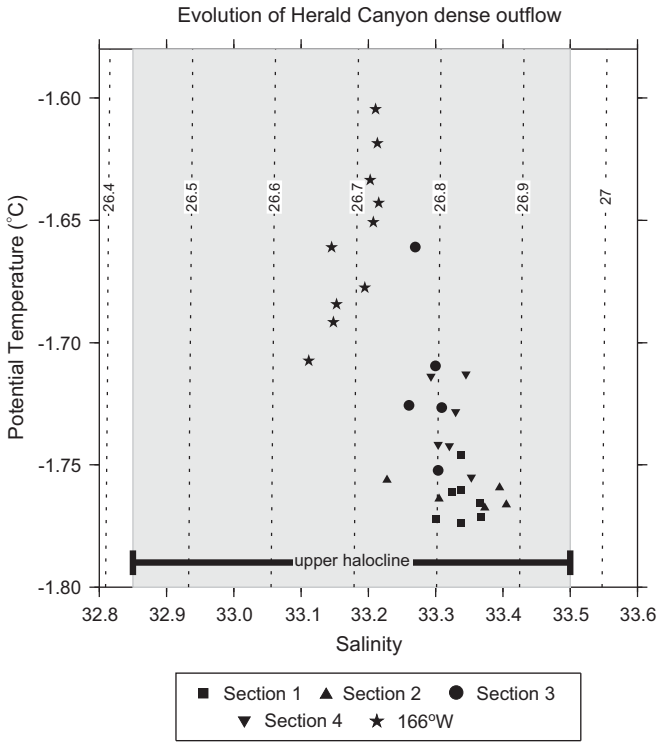

Fig. 17. Average T/S in the density range $26.6 \leq \sigma_\theta \leq 27.0$ (kg m^{-3}) for each of the Herald Canyon stations and the 166°W Chukchi slope stations (see key). The density range of the upper halocline from the historical data analyzed by Pickart (2004) is shaded gray.

of this, and the numerical models discussed above, it is difficult to imagine how either the winter water or summer water exiting Herald Canyon can progress directly offshore into the basin as a jet, as suggested by Steele et al. (2004). Rather, the flow seems to form an eastward-flowing boundary current, consistent with geostrophic dynamics. (Note that the transposition of the dense water to the eastern side of Herald Canyon is an important aspect of this scenario.) Nonetheless, it is clear that a significant fraction of the Pacific water does indeed escape into the basin interior. This is evident by the summer and winter water observed offshore (e.g. Shimada et al., 2001; Steele et al., 2004), and by the small value of eastward transport in the Beaufort shelfbreak jet versus the measured northward transport in Bering Strait (Nikolopoulos et al., 2009). However, it seems that turbulent processes, such as eddy formation (Pickart et al., 2005; Spall et al., 2008) may be the dominant mechanism for this off-shelf transport. While wind-driven flow from the frequent storms in the region may also play a significant role in fluxing the water offshore, this requires further investigation.

Acknowledgments

The authors acknowledge the Captain and crew of the *Professor Khromov*, as well as our Russian colleagues in the RUSALCA program and Group Alliance, for making the 2004 expedition a success. Special thanks goes to Marshall Swartz and Mark Dennett for their hard work in collecting the CTD and lowered ADCP data. This project was funded by the following agencies: The Climate Program Office of the National Oceanic and Atmospheric Administration, grant NA17RJ1223 (RSP and AYP) and NA17RJ1224 (TEW); the National Science Foundation, grant ARC-073248 (KA) and grant OCE-0525729 (LJP); the Natural Sciences and Engineering Research Council of Canada (GWKM). Additional support was provided by the National Defense Science and Engineering Graduate Fellowship program (HJD).

References

Aagaard, K., Roach, A.T., 1990. Arctic ocean-shelf exchange: measurements in Barrow Canyon. Journal of Geophysical Research 95, 18,163–18,175.
Barth, J.A., Bogucki, D., Pierce, S.D., Kosro, P.M., 1998. Secondary circulation associated with a shelfbreak front. Geophysical Research Letters 25, 2761–2764.
Cavalieri, D.J., Crawford, J.P., Drinkwater, M.R., Eppler, D.T., Farmer, L.D., Jentz, R.R., Wackerman, C.C., 1991. Aircraft active and passive microwave validation of sea ice concentration from the DMSP SSM/I. Journal of Geophysical Research 96, 21,989–22,008.
Cavalieri, D.J., Martin, S., 1994. The contribution of Alaskan, Siberian, and Canadian coastal polynyas to the cold halocline of the Arctic Ocean. Journal of Geophysical Research 99, 18,343–18,362.
Chapman, D.C., Lentz, S.J., 1994. Trapping of a coastal density front by the bottom boundary layer. Journal of Physical Oceanography 24, 1464–1479.
Chapman, D.C., 1999. Dense water formation beneath a time-dependent coastal polynya. Journal of Physical Oceanography 29, 807–820.
Chapman, D.C., 2000. The influence of an alongshelf current on the formation and offshore transport of dense water from a coastal polynya. Journal of Geophysical Research 105, 24,007–24,019.
Coachman, L.K., Aagaard, K., Tripp, R.B., 1975. In: Bering Strait: The Regional Physical Oceanography. University of Washington Press, Seattle, 172pp.
Codispoti, L.A., Richards, R.A., 1968. Micronutrient distributions in the East Siberian and Laptev Sea during summer, 1963. Arctic 21, 67–83.
Dalziel, S.B., 1988. Two-layer hydraulics: maximal exchange flows. Ph.D. Thesis, University of Cambridge, England.
D'Asaro, E.A., 1988. Observations of small eddies in the Beaufort Sea. Journal of Geophysical Research 93, 6669–6684.
Garrison, G.R., Becker, P., 1976. The Barrow submarine canyon: a drain for the Chukchi Sea. Journal of Geophysical Research 81, 4445–4453.
Gawarkiewicz, G.G., Chapman, D.C., 1992. The role of stratification in the formation and maintenance of shelf-break fronts. Journal of Physical Oceanography 22, 753–772.
Gawarkiewicz, G.G., 2000. Effects of ambient stratification and shelfbreak topography on offshore transport of dense water on continental shelves. Journal of Geophysical Research 105, 3307–3324.
Gawarkiewicz, G.G., Shcherbina, A., Charette, M., Graziano, L., 2009. Frontal upwelling and nutrient transport in the Shelfbreak Front of the Middle Atlantic Bight Nature Geoscience, submitted.
Gill, A.E., 1977. The hydraulics of rotating-channel flow. Journal of Fluid Mechanics 80, 641–671.
Houghton, R.W., Visbeck, M., 1998. Upwelling and convergence in the Middle Atlantic Bight shelf break front. Geophysical Research Letters 25, 2765–2768.
Hunkins, K., Whitehead, J.A., 1992. Laboratory simulation of exchange through Fram Strait. Journal of Geophysical Research 97 (C7), 11,299–11,321.
Kirillova, E.P., Stepanov, O.V., Weingartner, T.J., 2001. Distribution and variability of nutrients in the northwestern part of the Chukchi Sea. Proceedings of the Arctic Regional Centre 3, 107–115.
Kowalik, Z., Proshutinsky, A.Y., 1993. The diurnal tides in the Arctic Ocean. Journal of Geophysical Research 98, 16,449–16,468.
Kowalik, Z., Proshutinsky, A.Y., 1994. The Arctic Ocean tides. In: Johannessen, O., Muench, R.D., Overland, J.E., (Eds.), The Polar Oceans and Their Role in Shaping the Global Environment; The Nansen Centennial Volume, Geophysical Monograph Series, 85, pp. 137–158.
Llinas, L., Pickart, R.S., Mathis, J.T., Smith, S.L., 2009. Zooplankton inside an Arctic Ocean cold-core eddy: probable origin and fate. Deep-Sea Research II 56, 1290–1304.
Mathis, J.T., Pickart, R.S., Hansell, D.A., Kadko, D., Bates, N.R., 2007. Eddy transport of organic carbon and nutrients from the Chukchi shelf into the deep Arctic basin. Journal of Geophysical Research 112, C05011, doi:10.1029/2006JC003899.
Moore, G.W.K., Renfrew, I.A., 2002. An assessment of the surface turbulent heat fluxes from the NCEP-NCAR reanalysis over the western boundary currents. Journal of Climate 15, 2020–2037.
Mountain, D.G., 1974. Bering Sea Water on the north Alaskan shelf. Ph.D. Thesis, University of Washington, Seattle, WA, 153pp.
Muench, R.D., Schumacher, J.D., Salo, S.A., 1988. Winter currents and hydrographic conditions on the northern central Bering Sea shelf. Journal of Geophysical Research 93, 516–526.
Munchow, A., Carmack, E.C., 1997. Synoptic flow and density observations near an Arctic shelfbreak. Journal of Physical Oceanography 27, 1402–1419.
Nikolopoulos, A., Borenäs, K., Hietala, R., Lundberg, P.A., 2003. Hydraulic estimates of Denmark Strait overflow. Journal of Geophysical Research 108 (C3), 3095, doi:10.1029/2001JC001283.
Nikolopoulos, A., Pickart, R.S., Fratantoni, P.S., Shimada, K., Torres, D.J., Jones, E.P., 2009. The western Arctic boundary current at 152°W: structure, variability, and transport. Deep-Sea Research II 56, 1164–1181.
Overland, J.E., Hiester, R.T., 1980. Development of a synoptic climatology for the Northeast Gulf of Alaska. Journal of Applied Meteorology 19, 1–14.

Padman, L., Erofeeva, S., 2004. A barotropic inverse tidal model for the Arctic Ocean. Geophysical Research Letters 31, L02303, doi:10.1029/2003GL019003.
Pease, C.H., 1987. The size of wind-driven polynyas. Journal of Geophysical Research 92, 7049–7059.
Pickart, R.S., 2000. Bottom boundary layer structure and detachment in the shelfbreak jet of the Middle Atlantic Bight. Journal of Physical Oceanography 30, 2668–2686.
Pickart, R.S., 2004. Shelfbreak circulation in the Alaskan Beaufort Sea: mean structure and variability. Journal of Geophysical Research 109 doi:10.1029/2003JC001912.
Pickart, R.S., Weingartner, T.J., Pratt, L.J., Zimmermann, S., Torres, D.J., 2005. Flow of winter-transformed water into the western Arctic. Deep Sea Research II 52, 3175–3198.
Pickart, R.S., Moore, G.W.K., Macdonald, A.M., Walsh, J.E., Kessler, W.S., 2008. Seasonal evolution of Aleutian low-pressure systems: Implications for the North Pacific sub-polar circulation. Journal of Physical Oceanography 39, 1316-1339. [doi: 10.1175/2008JPO3891.1].
Pratt. L.J., 2008. Composite Froude numbers and critical conditions for layered flow with transverse variations in velocity. Journal of Fluid Mechanics 605, 281–291.
Pratt, L.J., Whitehead, J.A., 2008. In: Rotating Hydraulics. Springer, New York 589pp.
Proshutinsky, A.Y., 1993. In: Arctic Ocean Level Oscillations. Gidrometeoizdat, St. Petersburg 216pp.
Proshutinsky, A.Y., Johnson, M., 1997. Two circulation regimes of the wind-driven Arctic Ocean. Journal of Geophysical Research 102, 12,493–12,514.
Rabe, B., Smeed, D.A., Dalziel, S.B., Lane-Serff, G.F., 2007. Experimental studies of rotating exchange flow. Deep-Sea Research I 54, 269–291.
Rothrock, D.A., 1975. The mechanical behavior of pack ice. Annual Review of Earth and Planetary Sciences 3, 317–342.
Sannino, G., Pratt, L.J., Carillo, A., 2009. Hydraulic criticality of the exchange flow through the Strait of Gibraltar. Journal of Physical Oceanography, in press.
Shimada, K., Carmack, E.C., Hatakeyama, K., Takizawa, T., 2001. Varieties of shallow temperature maximum waters in the western Canadian basin of the Arctic ocean. Geophysical Research Letters 28, 3441–3444.
Smeed, D.A., 2000. Hydraulic control of three-layer exchange flows: application to the Bab al Mandab. Journal of Physical Oceanography 30, 2574–2588.
Smith, P.C., 1975. A streamtube model for bottom boundary currents in the ocean. Deep-Sea Research 22, 853–873.
Spall, M.A., 2007. Circulation and water mass transformation in a model of the Chukchi Sea. Journal of Geophysical Research 112, C05025, doi:10.1029/2005JC003364.
Steele, M., Morison, J., Ermold, W., Rigor, I., Ortmeyer, M., 2004. Circulation of summer Pacific halocline water in the Arctic Ocean. Journal of Geophysical Research 109, C02027, doi:10.1029/2003JC002009.
Spall, M.A., Pickart, R.S., Fratantoni, P.S., Plueddemann, A.J., 2008. Western Arctic shelfbreak eddies: formation and transport. Journal of Physical Oceanography 38, 1644–1668.
Weingartner, T.J., Cavalieri, D.J., Aagaard, K., Sasaki, Y., 1998. Circulation, dense water formation, and outflow on the northeast Chukchi shelf. Journal of Geophysical Research 103, 7647–7661.
Weingartner, T., Danielson, S., Sasaki, Y., Pavlov, V., Kulakov, M., 1999. The Siberian Coastal current: a wind- and buoyancy-forced Arctic coastal current. Journal of Geophysical Research 104 (C12), 29697–29713.
Weingartner, T., Aagaard, K., Woodgate, R., Danielson, S., Sasaki, Y., Cavalieri, D., 2005. Circulation on the north central Chukchi Sea shelf. Deep-Sea Research II 52, 3150–3174.
Whitehead, J.A., Leetmaa, A., Knox, R.A., 1974. Rotating hydraulics of strait and sill flows. Geophysical Fluid Dynamics 6, 101–125.
Whitledge, T.E., Malloy, S.C., Patton, C.J., Wirick, C.D., 1981. Automated nutrient analysis in seawater. Brookhaven National Laboratory Technical Report, BNL 51398.
Wilkinson, D.L., Wood, I.R., 1971. A rapidly varied flow phenomenon in a two-layer flow. Journal of Fluid Mechanics 47, 241–256.
Winsor, P., Björk, G., 2000. Polynya activity in the Arctic Ocean from 1958 to 1997. Journal of Geophysical Research 105 (C4), 8789–8803.
Winsor, P., Chapman, D.C., 2002. Distribution and interannual variability of dense water production from coastal polynyas on the Chukchi shelf. Journal of Geophysical Research 107.
Winsor, P., Chapman, D.C., 2004. Pathways of Pacific water across the Chukchi Sea: a numerical model study. Journal of Geophysical Research 109, C03002, doi:10.1029/2003JC001962.
Woodgate, R.A., Aagaard, K., Weingartner, T.J., 2005. A year in the physical oceanography of the Chukchi Sea: moored measurements from autumn 1990–1991. Deep-Sea Research II 52, 3116–3149.